Millennial Scale Impacts of Marine Biogenic Calcification Changes on Ocean Carbon

Cycling

Andrew Jason Pinsonneault

A Thesis

In the Department

of

Geography, Planning, and Environment

Presented in Partial Fulfillment of the Requirements

For the Degree of

Master of Science (Geography, Urban, and Environmental Studies)

At Concordia University

Montreal, Quebec, Canada

August 2011

CONCORDIA UNIVERSITY
School of Graduate Studies

This is to certify that the thesis prepared

By: Andrew Jason Pinsonneault

Entitled: Millennial Scale Impacts of Marine Biogenic Calcification Changes on Ocean Carbon Cycling

and submitted in partial fulfillment of the requirements for the degree of

Master of Science (Geography, Urban, and Environmental Studies)

complies with the regulations of the University and meets the accepted standards with respect to originality and quality.

Signed by the final Examining Committee:

_____David Greene_____   Chair
Dr. David Greene

_____Eric Galbraith_____   Examiner
Dr. Eric Galbraith

_____Alfonso Mucci_____   Examiner
Dr. Alfonso Mucci

_____Damon Matthews_____   Supervisor
Dr. Damon Matthews

Approved by   _____David Greene_____
                                    Dr. David Greene
                                    Chair of Department

August 09   2011   _____Brian Lewis_____
                                    Dr. Brian Lewis
                                    Dean of Arts & Science

ABSTRACT

Millennial Scale Impacts of Marine Biogenic Calcification Changes on Ocean Carbon Cycling

Andrew Jason Pinsonneault

Ocean acidification resulting from increasing anthropogenic carbon dioxide (CO_2) emissions are likely to impact calcification rates in pelagic organisms which may, in turn, lead to changes in the strength of the ocean carbon sink. However, the responses of pelagic calcifying organisms to acidification driven changes vary widely between species. This leads to a degree of uncertainty in predicting the future fate of anthropogenic CO_2 and the resulting climate change. Here, I address this uncertainty by introducing a dependence of calcium carbonate ($CaCO_3$) production on calcite saturation state (Ω_{CaCO3}) in the University of Victoria Earth System Climate Model, an intermediate complexity coupled carbon-climate model. In a series of model simulations, I examine the changes in global ocean carbon cycling following both "business-as-usual" and "mitigation" CO_2 emissions scenarios. By the year 3500, global $CaCO_3$ production rates will have decreased by between 0.003 Pg C y^{-1} and 0.264 Pg C y^{-1} relative to the standard model configuration depending on the sensitivity of calcification rates to Ω_{CaCO3}. This, in turn, would result in an atmospheric CO_2 drawdown of 0.630 – 59.8 Pg C, a weakening of the vertical ocean alkalinity and DIC gradients, and a change to sediment and ocean carbon pools of 1.00 – 42.0 Pg C and 0.800 to 70.0 Pg C respectively. These results suggest that the response of pelagic calcifying organisms to anthropogenically-driven changes in ocean Ω_{CaCO3} can have an important influence on marine biological carbon

cycling, leading to changes in carbon partitioning between the ocean and atmosphere on millennial timescales.

Acknowledgements/Dedication

First and foremost I would like to thank my supervisor, Dr. Damon Matthews, for his unerring support over the last two years and for recognizing and nurturing a potential in me I hadn't even known was there. I would not be where I am today were it not for him. I'd also like to thank Dr. Eric Galbraith for his guidance and patience over the last year despite my being a poor listener at times and Dr. Andreas Schmittner for being kind enough to provide the base code necessary to make the model developments required for my research.

Special thanks go out to Nathan Taylor, Elizabeth Le Maistre, Patric Gagner, Irkar Beljaars and Normand Crawford, members of my chosen family, for being there for me from the beginning. Words cannot express how grateful I am to all of them for going above and beyond the call of duty in their support, their patience, and keeping me sane when the stress was at its worst. This thesis would never have been successfully completed without them and so I dedicate this work to them.

Contribution of Authors

The authors listed below have certified* that:

1. they meet the criteria for authorship in that they have participated in the conception, execution, or interpretation, of at least that part of the publication in their field of expertise;
2. they take public responsibility for their part of the publication, except for the responsible author who accepts overall responsibility for the publication;
3. there are no other authors of the publication according to these criteria;
4. potential conflicts of interest have been disclosed to (a) granting bodies, (b) the editor or publisher of journals or other publications, and (c) the head of the responsible academic unit, and
5. they agree to the use of the publication in the student's thesis and its publication on the Australasian Digital Thesis database consistent with any limitations set by publisher requirements.

In the case of this chapter:

Biogenic Calcification Sensitivity and the Marine Carbon Cycle:

Contributor	Statement of contribution*
Andrew Pinsonneault August 09, 2011	Wrote the manuscript, experimental design, conducted experiments, and data analysis
Damon Matthews	Aided experimental design, data analysis
Eric Galbraith	Aided experimental design, data analysis
Andreas Schmittner	Aided with model code development

Principal Supervisor Confirmation

I have sighted email or other correspondence from all Co-authors confirming their certifying authorship.

Damon Matthews		August 09, 2011
Name	Signature	Date

Table of Contents

List of Figures

List of Tables

List of Equations

Chapter 1. Introduction

Increasing anthropogenic emissions of carbon dioxide (CO_2) to the atmosphere, resulting primarily from fossil fuel combustion and deforestation, is one of the greatest challenges facing the modern world due to the significant environmental and socio-economic impacts associated with the resulting changes in the global climate system. These changes include rising surface air temperatures (SAT) and ocean temperatures, changes to biogeochemical cycling of elements such as carbon, and modified ecosystem functioning which can have significant deleterious effects on ecosystem services, biodiversity, and trophic structures. Therefore, it is essential to accurately understand and thus predict the impacts of rising atmospheric CO_2 concentrations ($[CO_2]_{atm}$) on existing carbon sinks, which currently absorb more than half of anthropogenic CO_2 emissions (Le Quéré *et al*., 2009). The world oceans represent the largest reservoir of carbon that is exchanged with the atmosphere in the form of CO_2 on millennial timescales (Zondervan *et al*., 2001); understanding the sensitivity of this carbon sink to continued CO_2 emissions is critical in order to predict the fate of future $[CO_2]_{atm}$ and the extent of future climate change.

CO_2 is exchanged between the atmosphere and ocean at a rate of approximately 90 gigatonnes of carbon per year (Gt C yr^{-1}) (Falkowski *et al*., 2000), due to differences in the partial pressure of CO_2 (pCO_2) across the air-sea interface. As such, there are important feedbacks and interactions between changes in global climate, atmospheric chemistry and changes in the state of the ocean which can impact the strength of the

1

ocean as a carbon sink and, consequently, the rate and magnitude of global climate change (Hofmann & Schellnhuber, 2009; Secretariat of the Convention on Biological Diversity, 2009; hereafter SCBD, 2009). One such change in ocean state, which is an issue of growing concern in the scientific community, is that of ocean acidification due to the uptake of anthropogenic CO_2 (Denman *et al*., 2007). The measure used to define the intensity of the acidity of a solution is pH, which is defined as the log of the hydrogen ion concentration in solution (SCBD, 2009). Currently, on a scale of 0 to 14 where a pH < 7 is acidic, a pH = 7 is neutral, and a pH > 7 is basic, seawater has a pH of approximately 8 which is ~30% more acidic than preindustrial levels 250 years ago. It has been predicted that should $[CO_2]_{atm}$ increase by 0.5% - 1.0% per year throughout the 21st century, ocean acidity could increase by as much as 150% by 2100; this increase would occur 100 times faster than any change in ocean pH over the last 20 million years (SCBD, 2009).

As seen in Figure 1.1, the oceans regulate $[CO_2]_{atm}$ via two mechanisms: the solubility pump and two biological pumps: the organic carbon pump and the calcium carbonate ($CaCO_3$) counter-pump.
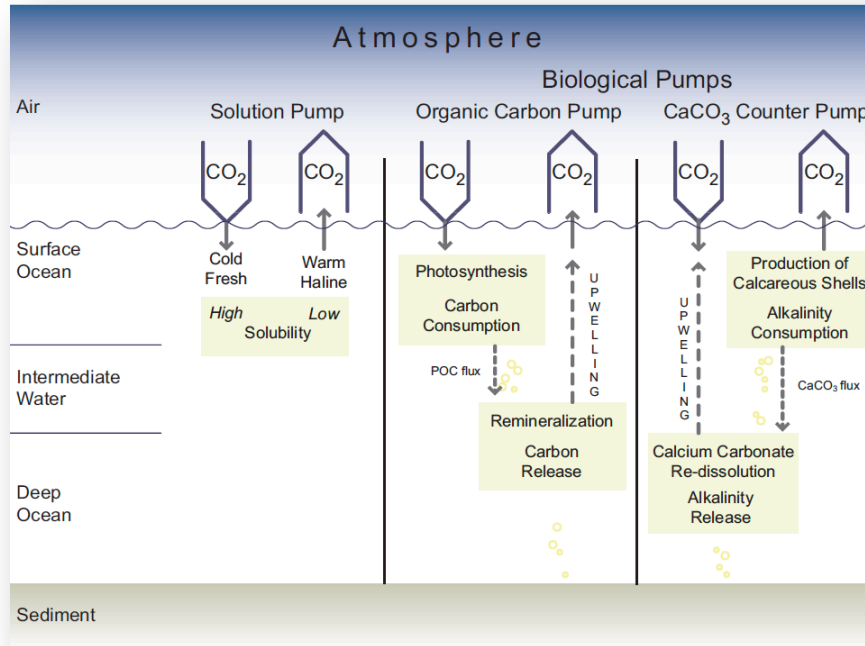
Figure 1.1 - The three main ocean carbon pumps governing atmospheric CO_2 regulation (Denman *et al.*, 2007, p. 530)

The solubility pump reflects the temperature dependence of the solubility of gaseous CO_2 in seawater (whereby CO_2 solubility increases with decreasing temperature) and the thermal stratification of the ocean (Ito & Follows, 2003). The organic carbon pump is driven by the primary production of marine phytoplankton in the euphotic zone, which converts dissolved inorganic carbon (DIC) and nutrients into particulate organic matter through photosynthesis:

$$6CO_2 + 6H_2O + Energy \rightarrow C_6H_{12}O_6 + 6O_2 \hspace{2cm} (1)$$

This particulate organic matter (e.g. in the form of detritus) is eventually exported from the surface euphotic zone to the deeper ocean.

The $CaCO_3$ counter-pump reflects changes in the release of surface water CO_2 during the formation of calcareous skeletons by calcifying marine life such as phytoplankton, molluscs, and corals, a process known as biogenic calcification. Biogenic calcification rates in turn depend (among other things) on the carbonate saturation state of the ocean, defined as:

$$\Omega = [Ca^{2+}]*[CO_3^{2-}]/K^*_{sp} \qquad\qquad (2)$$

Here, $[Ca^{2+}]$ and $[CO_3^{2-}]$ are the concentration of calcium and carbonate ions in seawater, and K^*_{sp}, which is dependent on temperature, pressure and salinity, is the stoichiometric solubility product for $CaCO_3$ (Mucci, 1983). Consequently, changes to surface ocean chemistry, such as the effect of ocean acidification on the availability of carbonate ions, or the effect of sea surface temperatures on solubility products and acid dissociation constants, have the potential to alter the carbonate saturation state (Ω_{CaCO3}) (Sarmiento & Gruber, 2006; SCBD, 2009; Takahashi *et al.*, 1993). This, in turn, will affect biogenic calcification rates, and hence could alter the strength of the ocean carbon sink (Raven & Falkowski, 1999; SCBD, 2009). However, the calcification response to acidification and changes in Ω_{CaCO3} varies widely between different species of calcifiers, which introduces a key uncertainty in future predictions of marine carbon cycling and climate change (Ridgwell *et al.*, 2006; Ilyina *et al.*, 2009).

CaCO$_3$-rich coastal and deep-sea sediments are also fundamental in regulating $[CO_2]_{atm}$. This occurs because organic and inorganic carbon deposited to the marine

sediments by the biological carbon pumps is very responsive to changes in the overlying

ocean chemistry (Ridgwell & Hargreaves, 2007). For example, ocean acidification can

cause $CaCO_3$-rich sediments to dissolve, thereby altering both the oceans' capacity to

buffer changes in ocean pH and promoting atmospheric CO_2 uptake (Gehlen *et al*., 2007).

This change in deep-sea sediments occurs on a millennial timescale because the

meridional overturning circulation, whereby surface water sinks to the deep ocean,

circulates at depth, and is eventually returned to the surface, operates on a timescale of

about 1000 years (SCBD, 2009). By comparison, marine coastal sediments are a more

rapidly reacting $CaCO_3$-reservoir in comparison to the deep-sea sediments because they

occur in more shallow waters and the dominant forms of $CaCO_3$ that are deposited in

these regions have a higher solubility than those found in deep-sea sediments (Morse *et*

al., 2006). Consequently, in order to reduce uncertainty about the fate of future

atmospheric CO_2 and climate change, marine sediment interactions must be considered in

long-term predictions.

1.1 Purpose of Study

The purpose of this study is to expand on the work conducted by Ridgwell *et al.* (2006), Ilynia *et al.* (2009), and Gangsto *et al.* (2011) by:

1) Incorporating a $CaCO_3$ production rate dependence on ocean $CaCO_3$ saturation state into an intermediate complexity climate model.

2) Exploring a range of calcification responses, reflecting experimental uncertainty in the biogenic calcification response to increasing ocean carbon uptake.

3) Assessing the resulting impact on the magnitude and direction of future marine carbon-climate feedbacks on millennial timescales.

The climate model used in this study is the University of Victoria Earth System Climate Model (UVic ESCM) version 2.9 – which consists of a climate model coupled with a number of sub-component models including a primitive equation three-dimensional ocean general circulation model, models of the marine organic and inorganic carbon cycles, and a marine sediment model component. Despite their having different solubilities and reaction kinetics, the UVic ESCM does not differentiate between the different polymorphs of $CaCO_3$, such as calcite or aragonite, therefore no such distinction shall be made in this study.

1.2 Research Question

How will adding a dependence of the $CaCO_3$ production rate on ocean calcite saturation state impact millennial scale model projections of the effects of ocean acidification on marine carbon cycling and the fate of anthropogenic CO_2 under a range of CO_2 emission scenarios and biogenic calcification responses?

Chapter 2. Literature Review

2.1 Marine Carbon Cycle

Much research has been conducted on marine carbon chemistry in order to improve our understanding of global carbon cycling resulting in a number of reviews and syntheses of the literature. For example, it is known that where cold and dense water masses sink into the deep ocean basins at high latitudes they entrain anthropogenic CO_2 at depth because the solubility of atmospheric CO_2 in seawater increases with decreasing water temperature. When atmospheric CO_2 is dissolved in seawater it dissociates into several species of dissolved inorganic carbon (DIC) which includes bicarbonate ion (HCO_3^-), carbonate ion (CO_3^{2-}), and aqueous CO_2 ($CO_2(aq)$) in an approximate ratio of 90:9:1 (Figure 2.1). DIC accumulates in the surface waters before being circulated to the deep ocean and back up again over the space of hundreds to a thousand years (Doney *et al.*, 2009; SCBD, 2009).
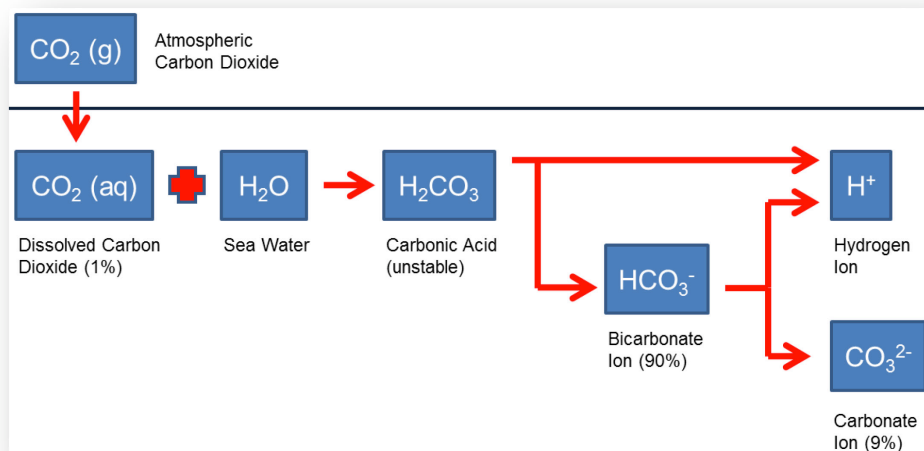
Figure 2.1 – The reaction between CO_2 and seawater (derived from Doney *et al.*, 2009)

As these bottom waters circulate from the Atlantic to the Indian and Pacific oceans they

accumulate more DIC from metabolic degradation of organic carbon on the sea floor. The

solubility pump is responsible for approximately 20% of the vertical ocean DIC gradient

where the DIC concentration ([DIC]) is 10-15% higher in deep waters than at the surface

(Sarmiento & Gruber, 2006; SCBD, 2009). It is the relative proportion of each of these

DIC species that govern seawater pH on short timescales.

The total alkalinity (ALK) of seawater is defined by Department of Energy (1994)

as:

$$\text{ALK} = [HCO_3^-] + 2[CO_3^{2-}] + [OH^-] + [B(OH)_4^-] + [HPO_4^{2-}] + 2[PO_4^{3-}] \hspace{1cm} (3)$$
$$+ [H_3SiO_4^-] + [NH_3] + [HS^-] - [H^+] - [HSO_4^-] - [HF] - [H_3PO_4]$$

where $[OH^-]$ is the hydroxide ion concentration (ccn), $[B(OH)_4^-]$ is the ccn of

tetrahydroxyborate ion, $[HPO_4^{2-}]$ is the ccn of hydrogen phosphate ion, $[PO_4^{3-}]$ is the ccn

of phosphate ion, $[H_3SiO_4^-]$ is the ccn of silicic acid, $[NH_3]$ is the ccn of ammonia, $[HS^-]$

is the ccn of hydrogen sulfide ion, $[H^+]$ is the ccn of free hydrogen ion, $[HSO_4^-]$ is the ccn

of hydrogen sulfate ion, $[HF]$ is the ccn of hydrogen fluoride, and $[H_3PO_4]$ is the ccn of

phosphoric acid. When the $[H^+]$ in seawater increases through processes like

anthropogenic ocean acidification, ions such as CO_3^{2-}, $B(OH)_4^-$, and OH^- act as proton

acceptors thereby buffering the ocean system to a certain extent against changes in pH

(Denman et al., 2007). The buffer factor, or Revelle factor , of seawater (Equation 4),

relates the fractional change in seawater pCO_2 to the fractional change in seawater DIC

after re-equilibration (Denman *et al.* 2007; Revelle & Suess, 1957; Sabine *et al.*, 2004;

Zeebe & Wolf-Gladrow, 2001).

Revelle Factor = $(\Delta[CO_2]/[CO_2]) / (\Delta[DIC]/[DIC])$ (4)

The value of the Revelle factor is proportional to the ratio of DIC:total alkalinity in the

surface ocean and the capacity of the ocean to uptake anthropogenic CO_2 is inversely

proportional to the Revelle factor (Sabine *et al.*, 2004). Consequently, increases in $[H^+]$

from ocean acidification lead to an increase in the DIC:alkalinity ratio which results in an

increase in both the Revelle factor and oceanic pCO_2 (Figure 2.2). This increase in

oceanic pCO_2, in turn, results in a reduced ability of the ocean to uptake anthropogenic

atmospheric CO_2.
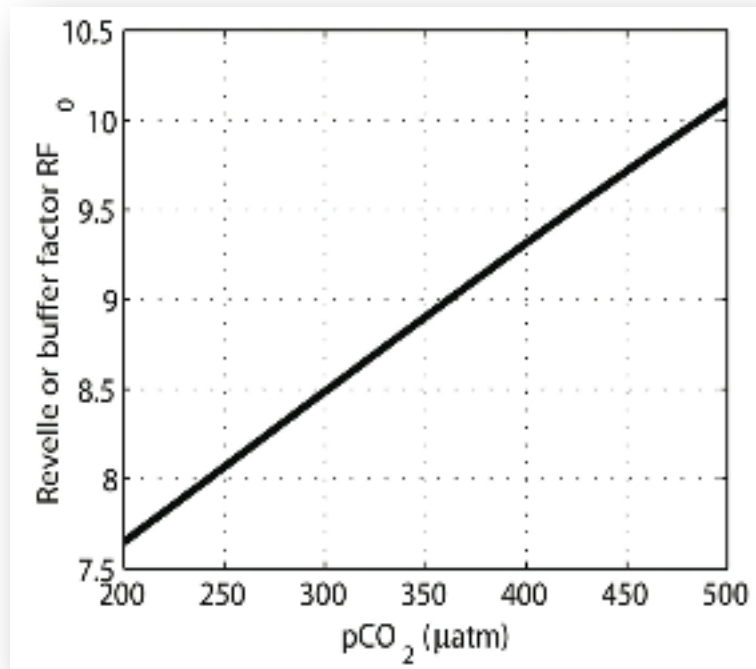
Figure 2.2 – The Revelle factor as a function of the CO_2 partial pressure for temperature 25°C, salinity 35 psu, and total alkalinity 2300 μmol kg^{-1} (Zeebe & Wolf-Gladrow, 2001, p.73)

It is important to note that increasing sea-surface temperature due to atmospheric CO_2-driven climate change stands to not only decrease the solubility of CO_2 in seawater but also to increase vertical ocean stratification thereby slowing down the vertical transport of DIC, nutrients, and alkalinity. This could significantly impact the ocean's capacity to uptake atmospheric carbon thus illustrating the importance of ocean chemistry in climate change research (SCBD, 2009).

According to the SCBD (2009), the organic carbon pump is estimated to contribute approximately 80% of the vertical ocean DIC gradient making this pump an integral part of the marine carbon cycle. In the organic carbon pump, photosynthetically-driven carbon uptake by phytoplankton in the euphotic zone fuels the export of

11

particulate organic carbon (POC), in the form of detritus, from the surface to the deeper

waters. Approximately 30% of this POC reaches deeper waters but most of it is

remineralized back into inorganic carbon in the water column by bacteria, thereby

contributing to the vertical DIC gradient, and only 0.1% of the POC actually reaches

ocean sediments where it accumulates. POC fluxes decrease rapidly in the ocean

thermocline (Sarmiento & Gruber, 2006) therefore the lower boundary of the thermocline

marks the locus of the POC remineralization horizon.

The carbonate counter-pump is primarily responsible for the vertical ocean

alkalinity gradient, though it also makes a very minor contribution to the vertical DIC

gradient. This pump is driven by calcium carbonate ($CaCO_3$) precipitation (calcification)

and dissolution. One way of representing the mechanism of calcification is presented in

Equation 5:

$$Ca^{2+} + 2HCO_3^- \; <-> \; CaCO_3 + H_2O + CO_2(aq) \qquad\qquad (5)$$
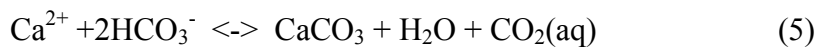
The precipitation of $CaCO_3$ results in an acidification of the solution through the release

of a small amount of CO_2 (aq) which, in turn, increases sea surface pCO_2 (and the

Revelle factor) and decreases the capacity of the upper ocean to uptake atmospheric CO_2.

Conversely, as illustrated in Figure 2.1, increased uptake of atmospheric CO_2 would

result in an increase in hydrogen ions (H^+) leading to reduced sea surface $[CO_3^{2-}]$ through

the formation of HCO_3^- impacting phytoplankton, shellfish, and coral calcification

(Barker *et al*., 2003; Doney *et al*., 2009; Gehlen *et al*., 2007; Hofmann & Schellnhuber,

2009; SCBD, 2009; Turley *et al.*, 2006; Tyrrell, 2008; Zondervan *et al.*, 2001). A reduction in biogenic calcification results in a greater increase in sea surface alkalinity than DIC which decreases both the Revelle factor and sea surface pCO_2 ultimately increasing the capacity of the ocean to uptake atmospheric CO_2. In other words, ocean acidification and reduced calcification have opposite effects on ocean CO_2 uptake capacity.

$CaCO_3$ exists in two primary forms: calcite, a form produced by calcifying phytoplankton such as coccolithophores and calcifying zooplankton such as foraminifera; and aragonite which is approximately 50% more soluble than calcite and is produced by mollusks and corals. Both coccolithophores and foraminifera have worldwide distributions though coccolithophores prefer warm, low-productivity areas so they are not a major component of marine phytoplankton in polar oceans (Dimiza *et al.*, 2011). Both coccolithophores and foraminifera use HCO_3^- as the substrate for calcification though foraminifera are also known to use $[CO_3^-]$ as a secondary substrate (Kuile *et al.*, 1989; Sarmiento & Gruber, 2006).

When sea surface calcifiers die, their calcite skeletons are exported out of the surface ocean layer into the deep ocean as particulate inorganic carbon (PIC). The solubility of $CaCO_3$ increases with decreasing temperature and more so with increasing pressure, therefore, approximately half the $CaCO_3$ exported from the surface ocean dissolves within the water column and never reaches the sediments (Sarmiento & Gruber, 2006). This change in solubility with depth results in a saturation horizon ($\Omega_{CaCO3} = 1$),

above which the water is saturated with $CaCO_3$ (favouring $CaCO_3$ formation) and below which the water is undersaturated with $CaCO_3$ (favouring its dissolution). Changes in the locus of the $CaCO_3$ saturation horizon also leads to changes in the locus of the $CaCO_3$ lysocline. The lysocline is defined as the depth below which the rate of $CaCO_3$ dissolution in marine sediments increases rapidly and its depth is broadly consistent with the depth of the saturation horizon. (Sarmiento & Gruber, 2006; Zeebe & Westbrock, 2003). The locus of the saturation horizon and lysocline depends on the nature of the $CaCO_3$ polymorph with both occurring at shallower depths for aragonite than calcite.

Waters are supersaturated with respect to $CaCO_3$ at $\Omega_{CaCO3} \geq 1$, while they are undersaturated with respect to $CaCO_3$ at $\Omega_{CaCO3} < 1$. At $\Omega_{CaCO3} \geq 1$, decreases in Ω_{CaCO3} nevertheless impacts calcification rates while at $\Omega_{CaCO3} < 1$, the seawater becomes corrosive and the shells and skeletons of calcifying organisms are increasingly prone to dissolution causing growing concern for the future of calcifying marine life should the trends in anthropogenic CO_2 emissions continue (Barker *et al*., 2003; Doney, 2009; Doney *et al*., 2009; Feely *et al*., 1988; Riebesell *et al*., 2000; SCBD, 2009; Zondervan *et al*., 2001). At a fixed [DIC], a decrease in pH decreases the carbonate ions concentration and leads to a shoaling of the $CaCO_3$ saturation horizon and lysocline towards the surface resulting in a decrease in the volume of waters saturated with respect to $CaCO_3$, and an increase in the volume of waters undersaturated with respect to $CaCO_3$. This leads to increased dissolution of $CaCO_3$ in sediments that are located below the new lysocline. Carbonate compensation, a process which becomes significant on timescales of 5000-14 000 years, results in the eventual re-establishment of a new alkalinity equilibrium

between sediment carbonate burial and the terrestrial alkalinity input from weathering through a shifting in the locus of the carbonate compensation depth (CCD). The carbonate compensation depth is defined as the depth where the sediments have virtually lost all their $CaCO_3$ due to dissolution (Sarmiento & Gruber, 2006; Sundquist, 1986; Archer *et al.*, 1997, 1998, Zeebe & Westbrock, 2003; Ridgwell & Hargreaves, 2007; Tyrrell, 2008). Studies have observed that changes to Ω_{CaCO3} have a profound effect on species-specific calcification rates and, consequently, on marine carbon uptake and future climate change thus making it critical to reduce uncertainty regarding calcification responses to anthropogenic perturbation (SCBD, 2009).

2.2 Ocean Acidification

In 2008, 155 scientists from 26 countries signed the Monaco Declaration, which urged world leaders to take immediate and urgent action to mitigate the effects of ocean acidification, and warned of the high costs of inaction for the continued provision of ocean goods and services (Monaco Declaration, 2008; SCBD, 2009). In 2009, a statement released by the Inter-Academy Panel on International Issues called for ocean acidification to be considered in the international climate debate and further recommending a 50% reduction in global CO_2 emissions by 2050 to stabilize acidification below critical limits (Inter-Academy Panel on International Issues, 2009; SCBD, 2009). Predictions of future reductions in ocean pH range from 0.3 – 0.5 by 2100 following any of the Intergovernmental Panel on Climate Change (IPCC) CO_2 emissions scenarios and 0.8 and 1.4 by 2300 following cumulative emissions of 5000 and 20 000 PgC respectively (Caldeira & Wickett, 2005). Predictions of such dangerous levels of acidification in the

next 100-300 years make it all the more critical for society to adequately and quickly plan for both the most probable and worst-case scenarios of ocean acidification and warming.

2.3 Phytoplankton Physiological Response

With the biogenic calcification response to anthropogenic perturbation being so uncertain, a number of laboratory and macrocosm studies have been conducted. Doney (2009) and Doney *et al*. (2009) conducted a review of such studies, which addressed the physiological responses of major marine life groups to ocean acidification. More specifically, these studies examined the calcification response of coccolithophores, foraminifera, mollusks, echinoderms, tropical corals, and coraline red algae, the photosynthesis response of coccolithophores, prokaryotes and sea grasses, and the reproduction response of mollusks and echinoderms. According to the results synthesized by Doney (2009) and Doney *et al*. (2009), a vast majority of species exhibited a negative calcification response, a positive photosynthetic response, and a negative reproductive response to ocean acidification. Nevertheless, it should be noted that among the few species of coccolithophores that did not exhibit a negative calcification response to acidification, a positive response, no response, and a non-linear parabolic response were observed suggesting substantial inter-species and strain variability (Figure 2.3).

Physiological response / Major group	Species studied	a	b	c	d
Calcification					
Coccolithophores[1]	4	2	1	1	1
Planktonic Foraminifera	2	2	–	–	–
Molluscs	4	4	–	–	–
Echinoderms[1]	3	2	1	–	–
Tropical corals	11	11	–	–	–
Coralline red algae	1	1	–	–	–
Photosynthesis[2]					
Coccolithophores[3]	2	–	2	2	–
Prokaryotes	2	–	–	1	–
Seagrasses	5	–	–	–	–
Nitrogen Fixation					
Cyanobacteria	1	–	1	–	–
Reproduction					
Molluscs	4	4	–	–	–
Echinoderms	1	1	–	–	–
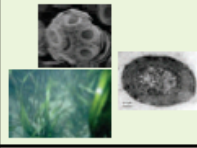
(Column header above a, b, c, d: Response to increasing CO_2)

1) Increased calcification had substantial physiological cost; 2) Strong interactive effects with nutrient and trace metal availability, light, and temperature; 3) Under nutrient replete conditions.

Figure 2.3 – Representative examples of impacts of ocean acidification on major groups of marine biota derived from experimental manipulation studies. (Doney *et al*., 2009, p.176)

To provide a quantitative example, Riebesell *et al.* (2000) chose to specifically examine the calcification response to acidification of coccolithophores because >80% of marine biogenic calcification is carried out by planktonic microorganisms, particularly coccolithophores. They conducted a laboratory experiment using two species of coccolithophore, *Emiliania huxleyi* and *Gephyrocapsa oceanica,* which are bloom forming and have worldwide distributions. Their results suggest that *E. huxleyi* and *G. oceanica* experience an increase in photosynthetic carbon fixation of 8.5% and 18.6%

respectively and a decrease in calcification of 15.7% and 44.7% respectively in response to changes in pH mimicking carbonate system responses to an atmospheric pCO_2 of 280 and 750 ppmv. The difference in the magnitude of the calcification response between *E. huxleyi* and *G. oceanica* further illustrates the uncertainty in coccolithophore calcification response to an increase in acidification.

2.4 Modeling of Biogenic $CaCO_3$ Production

Ocean acidification and its impact on marine carbonate chemistry has been a concern for many years and so there have been a number of modeling studies who set out to predict how rising atmospheric CO_2 and biogenic $CaCO_3$ production will interact in the future. The modern global $CaCO_3$ production rate is estimated at approximately 1 Pg C y^{-1} (Zondervan *et al*., 2001; Barker *et al.* 2003; Gangsto *et al*., 2011). Nevertheless, there are large uncertainties in this estimate and values range from 0.6-1.6 Pg C y^{-1} based on satellite and sediment-trap data and 0.4-1.8 Pg C y^{-1} based on model simulations (Doney *et al*., 2009).

Estimates of the reduction in biogenic $CaCO_3$ production in response to increasing atmospheric CO_2 has equally large uncertainties and varies widely between studies. Using the HAMOCC ocean model and ignoring the effects of climate change and ocean circulation, Heinze (2004) determined that between 1750 and 2250, biogenic $CaCO_3$ export production would decrease by approximately 50% following the Intergovernmental Panel on Climate Change (IPCC) A1B CO_2 emissions scenario up to the year 2100 and constant CO_2 emissions afterwards. This reduction in biogenic $CaCO_3$

18

production also resulted in a considerable shoaling of the organic carbon remineralization horizon. Andersson et al. (2006) used two basic biogeochemical box models following a "buisiness-as-usual" CO_2 emissions scenario and results suggested that, between 1700 and 2300, ocean acidification in conjunction with climate warming would reduce biogenic calcification by as much as 90%.

Gangsto et al. (2008) and Gehlen et al. (2007) both used the PISCES intermediate complexity model in their studies. Gangsto et al. (2008) used the IPCC SRES A2 CO_2 emissions scenario and predicted that, between 1861 and 2100, global biogenic $CaCO_3$ production would decrease by 19% while Gehlen et al. (2007) increased $[CO_2]_{atm}$ by 1% yr^{-1} over a 140-year time period and predicted that biogenic $CaCO_3$ production would decrease by 27% . This variation in the predicted reduction of biogenic $CaCO_3$ production illustrates the sensitivity of changes in biogenic $CaCO_3$ production to the atmospheric CO_2 emission trajectory employed as well as the complexity of the model used. These studies, however, were all conducted on centennial scales and therefore do not ultimately address carbon-climate feedbacks on the millennial timescale of the meridional overturning circulation.

2.5 Carbon Fluxes

Due to the export of both inorganic carbon and organic matter from the surface layer to the deeper ocean as well as large-scale ocean circulation, anthropogenic CO_2 perturbation of the surface layer has impacts on marine chemistry at depth. Changes to surface ocean photosynthesis and biogenic $CaCO_3$ production leads to changes in the flux

of both POC and particulate inorganic carbon (PIC) respectively which, in turn, strongly influence the vertical distribution of ocean DIC and alkalinity. This export ratio of POC as detritus and PIC as $CaCO_3$ is known as the rain ratio (Barker *et al.*, 2003). The actual ratio of PIC:POC from the surface region, however, is uncertain and estimates range from 0.17 to 0.4 (Wolf-Gladrow *et al.*, 1999; Zondervan *et al*, 2001).

Two hypotheses exist in the literature regarding how the rain ratio may change in response to climate-driven changes to ocean biogeochemistry. The first is that acidification/warming driven changes will decrease the PIC:POC rain ratio due to increased photosynthetic carbon uptake and decreased biogenic calcification, resulting in greater POC and reduced PIC export to the deep ocean respectively (Feely *et al.*, 2004; Orr *et al.*, 2005; Riebesell *et al.*, 2007; Wolf-Gladrow *et al.*, 1999; Zondervan *et al.*, 2001). For example, the results from a modeling study conducted by Barker *et al.* (2003) suggested that, if the rain ratio is allowed to change, a reduction in calcification leads to an increase in surface-ocean alkalinity which, in turn, acts as a negative feedback on rising atmospheric CO_2; in this case a reduction in $[CO_2]_{atm}$ of 5%. Zondervan *et al.*, 2001 took a slightly different approach and examined the rain ratio response on a species level using the coccolithophore species *E. huxleyi* and *G. oceanica*. Results of their laboratory study suggested that POC production increased and PIC production decreased for both species in response to acidification resulting in a decrease in PIC:POC of 21% - 31.5% for *E. huxleyi* and 44.7 - 52.5% for *G. oceanica* following different light treatments.

The second hypothesis is the ballast hypothesis, which suggests that most POC sinking below 1000m is ballasted by inorganic minerals such as opaline silica, lithogenic dust, and most especially PIC in the form of $CaCO_3$. In other words, at depth the fluxes of PIC and POC are suggested to be intimately related resulting in an asymptotic convergence so that changes in one would be mirrored in the other. This grants a high degree of predictive power to ballast mineral fluxes so that they can be used to predict POC fluxes at depths greater than 1000m. (Armstrong *et al.*, 2002; Armstrong *et al.*, 2009; Barker *et al.* 2003; De La Rocha & Passow, 2007; Doney *et al.*, 2009; Hofmann & Schellnhuber, 2009; Klass & Archer 2002; SCBD, 2009; Zondervan *et al.*, 2001). The mechanisms thought to be responsible for this include ballast minerals providing protection from remineralization to a fraction of POC exported from the surface layer to the deep ocean and that this fraction of POC acts as a "glue" for the sinking particle of PIC-POC thereby increasing its density and, consequently, it's sinking speed. The protected fraction of POC in a sinking particle will only be subject to remineralization when (and if) the protecting PIC fraction dissolves (Armstrong *et al.*, 2009). Ultimately, mineral ballasting increases the efficiency of the organic carbon pump. When Barker *et al.* (2003) included mineral ballasting in their modeling study, the ballast effect partially counteracted the increases in ocean uptake capacity caused by the reduction in calcification, enough to increase the fraction of CO_2 present in the atmosphere and surface ocean by 3 ppm and 3 μmol kg^{-1} respectively. This occurred because the simulated decrease in $CaCO_3$ export from the surface to the deep ocean resulted in a shoaling of the simulated POC remineralization horizon so that [DIC] in the surface and intermediate ocean increased thereby increasing the Revelle factor and ultimately acting

as a positive feedback on increasing $[CO_2]_{atm}$. Similar results were presented by Hofmann & Schellnhuber, (2009) who included mineral ballasting in their modeling study and predicted a lesser negative calcification feedback on increasing atmospheric CO_2 by approximately 60%.

2.6 Marine Sediments & Saturation State

Although shallow coastal-water carbonate sediments are a fast reacting carbon reservoir by comparison, deep-sea carbonate sediments can be viewed as a slow reacting carbon reservoir both connected to and interacting with the atmosphere over multiple turnover cycles of the meridional overturning circulation (Gehlen *et al*., 2008; Morse *et al*., 2006). Ridgwell & Hargreaves (2007) estimated that the average global burial rate of $CaCO_3$ in sediments was 0.121 PgC yr^{-1}, in good agreement with recent global carbonate budget estimates of 0.1-0.14 PgC yr^{-1} (Feely *et al*., 2004). They also estimated the mean surface sediment $CaCO_3$ content to be 32.5 % by weight, in agreement with both the 31.1 % by weight estimate by Eby *et al*. (2009) and observational estimates of 34.8 % by weight (Ridgwell & Hargreaves, 2007). Furthermore, Ridgwell & Hargreaves (2007) demonstrated the importance of the inclusion of ocean sediment interactions in predictions of future climate change and the fate of future anthropogenic CO_2 by showing that an additional 12 % of CO_2 emissions (223 ppm) were sequestered in the ocean as a result of reaction with deep-sea carbonate sediments on a timescale of 1.7 Kyrs, a shorter timescale than previously predicted for ocean sediment interactions.

22

For marine sediments in contact with overlying waters where the $\Omega_{CaCO3} \geq 1$, $CaCO_3$ dissolution in these sediments is induced by the release of CO_2 (aq) into the sediment pore waters as a result of organic matter respiration; a process called metabolic dissolution. For sediments in contact with overlying waters where the $\Omega_{CaCO3} < 1$, both the corrosiveness of the $CaCO_3$ undersaturated bottom waters as well as metabolic dissolution drive the dissolution of sediment $CaCO_3$ (Archer & Maier-Reimer, 1994; Gehlen *et al*., 2008). As such, water masses become increasingly enriched in metabolic CO_2 (aq) as they flow along the path of the meridional overturning circulation (MOC) (Figure 2.4) (Gehlen *et al*., 2008). It is important to note here, however, that there is still a degree of mixing between water masses travelling along the path of the MOC and that these water masses are not as discreet as they appear in Figure 2.4.
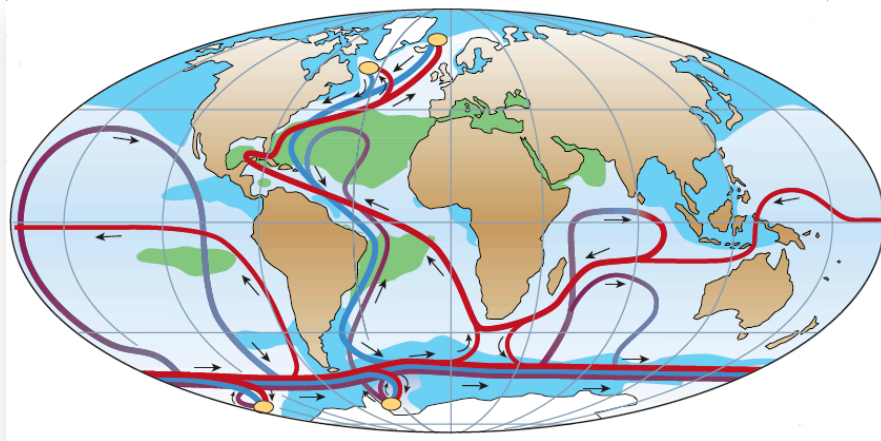
Figure 2.4 – Schematic of the meridional overturning circulation indicating warm surface waters (red), cold deep waters (blue), and deep water formation (yellow circles) (Rahmstorf, 2002, p. 208)

The youngest and least corrosive waters that were most recently in contact with the atmosphere are located in the Atlantic Ocean while the oldest and most corrosive waters,

which have slowly accumulated respired CO_2 (aq), are found in the Pacific Ocean (Zeebe & Zachos, 2007). Therefore, it logically follows that the regional $CaCO_3$ saturation state of the ocean is not uniform across the globe. Rather, the calcite lysocline is situated at 400 m, 2300 m, and 4200 m in the Pacific, Indian, and Atlantic Oceans respectively while aragonite lysocline is situated at 400 m, 1000 m and 3200 m in the Pacific, Indian, and Atlantic Oceans respectively (Gangsto *et al.*, 2008). Consequently, the relative area of the sea floor covered by $CaCO_3$-rich sediments is greater the North Atlantic and much smaller in the North Pacific thus showing a heterogeneous global spatial distribution (Gehlen *et al.*, 2008).

Between the preindustrial era and current day, the calcite saturation horizon has already shoaled by 40-100m N of 20°N in the North Pacific (Feely *et al.*, 2004). Consequently, numerous modeling studies have attempted to predict future changes in ocean saturation state and sediment dissolution. Using a box model, Andersson *et al.* (2006) predicted that the global average saturation state with respect to calcite would decrease by 73% by the year 2300 following a "business-as-usual" CO_2 emissions scenario while dissolution of carbonate minerals would increase by 267%. Using a similar model, Lenton & Britton (2006) predicted that changes in saturation state caused by cumulative anthropogenic CO_2 emissions $\geq$ 7350 GtC would dissolve all $CaCO_3$ in ocean sediments. This is broadly consistent with results from sediment core samples that suggest that >>2000 Pg C was dissolved in the ocean during the Paleocene-Eocene Thermal Maximum (PETM) resulting in a shoaling of the carbonate compensation depth of >2 Km and widespread dissolution of $CaCO_3$ in ocean sediments in only a few

thousand years (Zachos *et al*., 2005). However, ≥ 7350 GtC in cumulative anthropogenic CO_2 emissions exceeds even the increase in atmospheric carbon during the PETM and is emitted on a shorter timescale than the millennial-scale mixing time of the ocean suggesting that such emissions would result in even greater impacts on marine biota and ocean carbonate chemistry.

Orr *et al.* (2005) also used a "business-as-usual" CO_2 emissions scenario but, instead of using a box model, they used 13 uncoupled ocean models. Their results predicted that if atmospheric pCO_2 exceeded 600 ppm, reached at approximately year 2100, most of the southern oceans would become undersaturated with respect to aragonite with the saturation horizon shoaling from 730m to the surface, while in the North Atlantic above 50° the saturation horizon would shoal from 2600m to 115m . Less pronounced changes in the calcite saturation state were observed, however, with the saturation horizon remaining below 2200m. A number of studies have also been conducted using more advanced intermediate complexity coupled carbon-climate models and there is agreement that should atmospheric pCO_2 exceed 650 ppm most of the southern ocean would become undersaturated with respect to aragonite although even a modest stabilization of anthropogenic CO_2 emissions at 450 ppm would still result in enough of a shoaling of the saturation horizons that most of the deep ocean would become undersaturated with respect to both forms of $CaCO_3$ (Caldeira & Wickett, 2005; Cao *et al*., 2007; Cao & Caldeira, 2008). This is also supported by Gehlen *et al*. (2008) who predicted that with an increase in atmospheric pCO_2 from 286 ppm to 1144 ppm over 140 years, the total area of seafloor bathed by undersaturated bottom waters would

increase by 58%. With such drastic predicted changes in saturation state and sediment interactions on a centennial scale it follows that ocean biology, sediment, and terrestrial weathering responses to anthropogenic CO_2 perturbation remain even more uncertain on a millennial timescale (Eby *et al.*, 2009).

2.7 Climate Change

With marine carbon cycling and climate change being so intimately related, quantifying the extent and magnitude of their interaction is critical. Modeling studies agree that future climate change will result in increased sea surface temperature (SST) and ocean stratification (Cao *et al*., 2007; Chuck *et al*., 2005; Orr *et al.*, 2005; Ridgwell & Hargreaves, 2007, Riebesell *et al*., 2007; SCBD, 2009; Tyrell, 2008). Sea surface temperature affects ocean carbonate chemistry because the $CaCO_3$ solubility product, K^*_{sp}, and dissociation constants for carbonic acid, K'_1 for carbonic acid to bicarbonate and K'_2 for bicarbonate to carbonate respectively, all vary with temperature (Sarmiento & Gruber, 2006; SCBD, 2009; Takahashi *et al*., 1993) thus affecting Ω_{CaCO3}, sediment interactions, and biogenic calcification. In addition, sea surface temperature governs the solubility of atmospheric CO_2 in seawater (Cao *et al*., 2007; Matthews *et al*., 2009). Increases in sea surface temperature resulting from global warming may prolong phytoplankton growing seasons and open up new phytoplankton habitats (Tyrell, 2008). Increased ocean stratification, however, stands to decrease the availability of surface nutrients brought up from the deep-ocean thus having a negative impact on surface net primary productivity (NPP) by weakening ocean overturning circulation (Riebesell *et al*., 2007). Cao *et al.* (2007), however, determined that the effects of climate warming on

ocean carbon cycling were small compared with the direct effect of elevated CO_2 with climate warming resulting in an additional decrease in pH of 0.01 and 0.04 and a decrease in $\Omega_{aragonite}$ of 0.11 and 0.23 using climate sensitivities of 2.5° and 4.5° respectively and following an atmospheric pCO_2 stabilization at 1000 ppm.

Although it has been suggested that climate warming has only a small direct impact on ocean pH and saturation state, secondary impacts cannot be ignored. For example, Lenton & Britton (2006) have suggested that increased terrestrial weathering of carbonate and silicate minerals, on scales of $10^3 – 10^4$ years and $10^4 – 10^6$ years respectively, would increase alkalinity input into the ocean thereby decreasing the seawater Revelle factor via a shift in the seawater ratio of DIC:ALK and, consequently, accelerating long-term CO_2 uptake by a factor of 1.5 – 2.5 times with anthropogenic CO_2 emissions between 1100-4000 GtC and by a factor of 4 for emissions exceeding 7350 GtC. Schmittner et $al.$ (2008) further outlined the importance of climate change by predicting an increasing contribution of ocean-carbon cycle feedbacks to changes in biological carbon cycling over time with 24% and 38% of changes in biological carbon cycling resulting from climate-driven feedbacks by the years 2300 and 3000 respectively following a "business-as-usual" CO_2 emissions scenario. It should be noted, however, that Schmittner et al. (2008) did not account for the impacts of ocean acidification on carbon-climate feedbacks and the authors stress that the effect of ocean acidification on carbon-climate feedbacks on greater than century timescales remains to be quantified.

2.8 Calcification Response Scenarios

Three studies have previously attempted to address the uncertainty in biogenic

calcification response to anthropogenically driven ocean acidification. Using the

intermediate complexity coupled carbon-climate model GENIE-1 and Zhong & Mucci

(1993)'s mathematical description of the inorganic precipitation of carbonate, Ridgwell *et*

al. (2006) conducted a suite of model simulations to estimate the relative change in

$CaCO_3$ production in response to acidification for five phytoplankton species, corals, and

a mixed assemblage of these calcifiers. Assuming that existing conventional fossil fuel

reserves, estimated at 4000 PgC, would be used up by the early 24th century, Ridgwell *et*

al. (2006) predicted that there would be a substantial reduction in marine carbonate

production and an increase in ocean CO_2 sequestration of 62-199 PgC by the year 3000.

In terms of carbon-climate feedbacks, Ridgwell *et al.* (2006) found that increased ocean

surface temperature and increased stratification together actually enhanced sequestration

of atmospheric CO_2 resulting from reduced biogenic calcification by up to one third.

However, it should be noted that Ridgwell *et al.* (2006) did not account for $CaCO_3$

sediment interactions in quantifying the CO_2-calcification feedback, thus neglecting an

important component of marine carbon cycling on millennial scales.

The second study was conducted by Ilynia *et al.* (2009) who, using the HAMOCC

ocean general circulation model driven by the IPCC IS92a CO_2 emissions scenario,

examined the effects of changes in $CaCO_3$ production between the years 1800 and 2300

on ocean alkalinity through multiple calcification scenarios. These scenarios ranged from

a linear decrease in calcification rate with a $[CO_3^{2-}]$ of up to 80% for a 40% reduction in

$\Omega_{calcite}$ to a parabolic decrease in calcification rate as has been observed in coral species (Figure 2.5) (Ilyina *et al.*, 2009). Ilyina *et al.* (2009) found that ocean alkalinity stands to increase by 5-30 µmol kg^{-1} compared to present-day values by the year 2300, although changes to alkalinity resulting from changes in biogenic calcification won't start being detectable until the year 2040, with the largest predicted changes in surface ocean alkalinity in the tropical and subtropical regions.
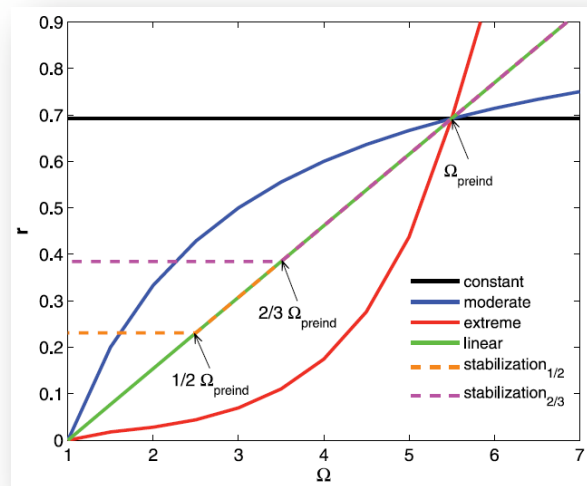
Figure 2.5 – Scenarios of biogenic calcification response to changes in saturation state (Ω). Calcification rate dependency on Ω is parameterized by the calcification rate coefficient (r). Arrows indicate changes in Ω with respect to preindustrial values (Ilyina *et al.*, 2009, p.3)

The third study was conducted by Gangsto *et al.* (2011) who carried out a sensitivity study using the biogeochemical Bern3D/PISCES model driven by a range of CO_2 emissions scenarios from the Intergovernmental Panel on Climate Change's suite of Representative Concentration Pathways, with different parameterizations of $CaCO_3$ production fitted to available laboratory and field data. Results from all model configurations showed a decrease in $CaCO_3$ production from approximately 1 Pg C y^{-1} to

between 0.36 and 0.82 Pg C y^{-1} by the year 2100. Overall, changes in $CaCO_3$ production/dissolution provided only a small reduction in atmospheric pCO_2 of approximately 1 to 11 ppm by the year 2100. Although the studies conducted by both Ilyina *et al.* (2009) and Gangsto *et al.* (2011) provide an indication of how ocean $CaCO_3$ production and, in turn, alkalinity may change in the coming centuries in response to rising $[CO_2]_{atm}$, changes to the deep ocean due to atmospheric changes occur on millennial scales and therefore studies examining longer time-scales are required.

2.9 Research in Context

The aims of my research are twofold. The first is to make a contribution towards model development by incorporating a $CaCO_3$ production rate dependence on calcite saturation state in a model in order to allow for more realistic treatment of the biogenic calcification response to anthropogenic perturbation. The second is to reduce the uncertainty in climate model predictions of the biogenic calcification response to climate change and the invasion of anthropogenic CO_2 in the world oceans, the resulting changes in marine carbon cycling, and the fate of anthropogenic CO_2. In this study, I expand on the work conducted by Ridgwell *et al.* (2006), Ilyina *et al.* (2009) and Gangsto *et al.* (2011) by examining these myriad and interconnected processes on millennial timescales using an updated intermediate complexity climate model with an active marine sediment component and including the effects of climate change. This will not only allow for the analysis of how these processes change while anthropogenic CO_2 is emitted but how the ocean carbon system recovers after said emissions have stopped and the meridional overturning circulation has gone through a full cycle bringing surface waters at the time

of peak CO_2 emissions down to the deep ocean and back up to the surface. Furthermore, I assess the changes to the marine carbon cycle under two CO_2 emissions scenarios, a "business-as-usual" scenario where atmospheric pCO_2 reaches a peak of 860 ppm and a "mitigation" scenario where atmospheric pCO_2 doesn't exceed 480 ppm, allowing me to quantify the environmental and biogeochemical change that could be avoided were we to drastically reduce our dependence on fossil fuels.

Chapter 3. Manuscript

Sensitivity of the Marine Carbon Cycle to Ocean Acidification and Changes in Biogenic Calcification

Running Title: Biogenic Calcification Sensitivity and the Marine Carbon Cycle

Andrew J. Pinsonneault[1]*, H. Damon Matthews[1], Eric Galbraith[2], Andreas Schmittner[3]

[1]Department of Geography, Planning and Environment,

Concordia University,

1455 de Maisonneuve Blvd W.,

Montreal, QC,

Canada, H3G 1M8

[2]Department of Earth & Planetary Sciences

McGill University

3450 University

Montreal, Qc

Canada, H3A 2A7

³College of Oceanic and Atmospheric Sciences

Oregon State University

104 COAS Administration Building

Corvallis OR 97331-5503

USA

*Corresponding author: *andr_pin@live.concordia.ca*, Phone: (514) 848-2424 x.2022,

Fax: 514-848-2032

Keywords: Biological Pump, Calcification, Carbon Cycle, Ocean Acidification, $CaCO_3$

Abstract

Ocean acidification resulting from increasing anthropogenic carbon dioxide (CO_2) emissions are likely to impact calcification rates in pelagic organisms which may, in turn, lead to changes in the strength of the ocean carbon sink. However, the responses of pelagic calcifying organisms to acidification driven changes vary widely between species. This leads to a degree of uncertainty in predicting the future fate of anthropogenic CO_2 and the resulting climate change. Here, we address this uncertainty by introducing a dependence of calcium carbonate ($CaCO_3$) production on calcite saturation state (Ω_{CaCO3}) in the University of Victoria Earth System Climate Model, an intermediate complexity coupled carbon-climate model. In a series of model simulations, we examine the changes in global ocean carbon cycling following both "business-as-usual" and "mitigation" CO_2 emissions scenarios. By the year 3500, global $CaCO_3$ production rates will have decreased by between 0.003 Pg C y^{-1} and 0.264 Pg C y^{-1} relative to the standard model configuration depending on the sensitivity of calcification rates to Ω_{CaCO3}. This, in turn, would result in an atmospheric CO_2 drawdown of 0.630 – 59.8 Pg C, a weakening of the vertical ocean alkalinity and DIC gradients, and a change to sediment and ocean carbon pools of 1.00 – 42.0 Pg C and 0.800 to 70.0 Pg C respectively. These results suggest that the response of pelagic calcifying organisms to anthropogenically-driven changes in ocean Ω_{CaCO3} can have an important influence on marine biological carbon cycling, leading to changes in carbon partitioning between the ocean and atmosphere on millennial timescales.

3.1 Introduction

Ocean uptake of atmospheric carbon dioxide (CO_2) is having a profound effect on biochemical cycles and ocean ecosystems. Increased CO_2 dissolution in the surface ocean leads to a decrease in seawater pH which is defined as the log of the hydrogen ion concentration in solution and which falls on a scale of 0 to 14 where a pH < 7 is acidic, a pH = 7 is neutral, and a pH > 7 is basic (SCBD, 2009). This, in turn, leads to a decrease in carbonate ion concentration ($[CO_3^{2-}]$), a shoaling of the calcium carbonate ($CaCO_3$) saturation horizon and lysocline, and an alteration of $CaCO_3$ stored in deep-sea sediments. This process, known as ocean acidification, has the potential to severely impact the biological carbon pumps, which influence the vertical alkalinity and dissolved inorganic carbon (DIC) gradients in the ocean. This, in turn, would affect the strength of the ocean as a carbon sink and, ultimately, the rate and magnitude of global climate change.

Biogenic calcification describes the formation of $CaCO_3$ by certain species of marine biota that use $CaCO_3$ to create their shells and skeletons (Doney *et al.*, 2009; Secretariat of the Convention on Biological Diversity, 2009; hereafter SCBD, 2009). In general, the rate of biogenic calcification depends on the saturation state of $CaCO_3$ in the surface ocean defined as:

$$\Omega_{CaCO3} = [Ca^{2+}][CO_3^{2-}]/K^*_{sp}$$

where $[Ca^{2+}]$ is the calcium ion concentration and K^*_{sp} is the stoichiometric solubility product which is dependent on temperature, salinity, and pressure. Studies have reported a decrease in biogenic calcification in response to decreasing calcium carbonate saturation state. Furthermore, modeling studies have predicted significant future reductions in ocean Ω_{CaCO3} caused by anthropogenic ocean acidification. This results in many areas in the water column, particularly the high-latitude oceans, becoming undersaturated with respect to calcite and/or aragonite, two different polymorphs of $CaCO_3$ (Caldeira & Wickett, 2005; Orr *et al*, 2005; Andersson *et al*., 2006; Lenton & Britton, 2006; Cao *et al*., 2007; Cao & Caldeira, 2008).

Calcifying marine life, such as cocolithophores and foraminifera, may be vulnerable to those predicted changes in Ω_{CaCO3} brought on by ocean acidification (Barker *et al*., 2003; Doney *et al*., 2009; Gehlen *et al*., 2007; Hofmann & Schellnhuber, 2009; SCBD, 2009; Turley *et al*., 2005; Tyrell, 2008; Zondervan *et al*., 2001). However, there is large variability in the calcifying response to acidification between species (Doney, 2009; Doney *et al*., 2009; Fabry *et al*., 2008; Guinotte & Fabry, 2008; Riebesell *et al*., 2000; Riebesell *et al*., 2007; Iglesias-Rodriguez *et al*., 2008). Decreased biogenic calcification ultimately leads to an increased ocean uptake of anthropogenic atmospheric CO_2 and a negative feedback on rising CO_2 levels offsetting the decreased ocean CO_2 uptake capacity resulting from acidification (Hofmann & Schellnhuber, 2009; Raven & Falkowski, 1999; Zondervan *et al*., 2001; Feely *et al*., 2004; Orr *et al*., 2005; Gehlen *et al*., 2008; Doney *et al*., 2009; Gangsto *et al*., 2011); however, the variability in species

specific responses introduces a large uncertainty to predictions of how this feedback will

operate in the future.

The ocean carbon cycle is clearly a critical component of the Earth system's

response to anthropogenic CO_2 emissions. The oceans have taken up approximately 30-

40% of anthropogenic CO_2 in the last 200 years (Raven & Falkowski, 1999; Feely *et al*.,

2004; Sabine *et al*., 2004; Zeebe *et al*., 2008) with an estimated daily uptake of 6 million

tons of carbon (Feely *et al*.,2008). Increased atmospheric CO_2 concentrations ($[CO_2]_{atm}$)

leads to an increase in surface ocean pCO_2. This, in turn, decreases $[CO_3^{2-}]$ and Ω_{CaCO3},

thereby hindering $CaCO_3$ production and facilitating $CaCO_3$ dissolution. As $CaCO_3$

production uses up 2 moles of alkalinity and 1 mole of DIC (Gangsto *et al*., 2011), a

reduction in production would lead to a greater increase in surface water alkalinity than

DIC; this, in turn, would result in a decrease in the Revelle factor of the surface ocean

and a greater oceanic capacity to uptake atmospheric CO_2. The Revelle factor, or buffer

factor, of the ocean describes how the pCO_2 of seawater changes for a given change in

[DIC] and its value is proportional to the ratio of sea surface DIC:alkalinity. As such, the

ocean capacity to uptake atmospheric CO_2 is inversely proportional to the Revelle factor

(Sabine *et al*., 2004). Neglecting mineral ballasting, a reduction in calcification may also

reduce the rain ratio of particulate inorganic carbon to particulate organic carbon

(PIC:POC) reaching the sediments. This would lead to greater metabolic dissolution of

sedimentary $CaCO_3$, brought on by the increased organic matter decomposition

acidifying sediment pore water, further altering of the vertical alkalinity and DIC

gradients as well as the strength of the ocean as a carbon sink (Barker *et al*., 2003; Feely

et al., 2004; Orr *et al*., 2005; Riebesell *et al*., 2007; Wolf-Gladrow *et al*., 1999;

Zondervan *et al*., 2001). Changes in deep ocean saturation state brought on by the

invasion of anthropogenic CO_2 in the deep ocean can also directly enhance the

dissolution of $CaCO_3$ in sediments (Lenton & Britton, 2006). This increased dissolution

of sedimentary $CaCO_3$ adds alkalinity to the ocean thereby reducing sea surface pCO_2

and further stimulating ocean carbon uptake on millennial timescales (Ridgwell &

Hargreaves, 2007).

Several recent modeling studies have been conducted to examine changes in

$CaCO_3$ production rates and their effect on the fate of anthropogenic CO_2 (Heinze, 2004;

Andersson *et al*., 2006; Gehlen *et al*., 2007; Gangsto *et al*., 2008). Despite significant

research attention, however, estimates of the current rate of global $CaCO_3$ production

vary widely: from 0.4 to 1.8 Pg C y^{-1} (Doney *et al*., 2009). Estimates of the calcification

response to ocean acidification are even more uncertain. For example, Gangsto *et al*.

(2008) simulated a 19% calcification decrease by 2100 in an intermediate complexity

climate model. In contrast, Andersson *et al*. (2006) simulated a 90% decrease in

calcification by 2300, using a box model driven by "business-as-usual" CO_2 emissions.

Much of this variability is attributed to the calcifying species represented in the model,

most often the cocolithophore Emiliania *huxleyi*. Consequently, other modeling studies

have sought to address the inter-species/strain uncertainty in calcification response by

comparing different calcification response scenarios. These studies have found that

increased sensitivity of $CaCO_3$ production to changes in Ω_{CaCO3} resulted in increased sea

surface alkalinity (Ilynia *et al*., 2009), increased carbon sequestration, and decreased

39

atmospheric pCO_2 (Ridgwell *et al*., 2006; Gangsto *et al*., 2011). Although studies agree that the calcification-CO_2 feedback is relatively small, on a scale ranging from 1 - 17.4 ppm CO_2 (Zondervan *et al*., 2001; Ridgwell *et al*., 2006; Gangsto *et al*., 2011), it still contributes uncertainty to climate model predictions. Consequently, it is critical that this feedback be properly represented in modeling studies, especially on centennial and longer timescales. It is also important to note that most modeling studies addressing the calcification-CO_2 feedback uncertainty are either conducted on centennial timescales or omit deep-sea carbonate sediment dynamics and so longer-term studies using models with deep-sea sediment components are required.

The purpose of this study is to expand on the work of Ridgwell *et al*. (2006), Ilynia *et al*. (2009), and Gangsto *et al*. (2011) by: 1) incorporating a $CaCO_3$ production rate dependence on ocean calcite saturation state into an intermediate complexity climate model; 2) exploring a range of calcification responses, reflecting experimental uncertainty in the biogenic calcification response to increasing ocean carbon uptake; and 3) assessing the resulting impact on the magnitude and direction of future ocean carbon-climate feedbacks on millennial timescales. We conduct a series of model simulations, following two 21st century CO_2 emissions scenarios, and continue the simulations until the year 3500 following a cessation of anthropogenic CO_2 emissions after 2100. These response scenarios are compared to the standard version of the model in order to determine the impact of changing marine calcification on ocean chemistry and the uptake of anthropogenic CO_2 on millennial timescales.

3.2 Materials & Methods

3.2.1 Model Description

The University of Victoria Earth System Climate Model (UVic ESCM) version 2.9 is an intermediate complexity global climate model with a spherical grid resolution of 1.8˚ latitude by 3.6˚ longitude. The climate component of the model consists of a simplified energy-moisture balance atmospheric model with dynamical feedbacks, coupled to a primitive equation three-dimensional ocean general circulation model (Modular Ocean Model 2 or MOM2), and a thermodynamic/dynamic sea ice model (Weaver *et al.*, 2001). The carbon cycle component of the model is represented by a dynamic vegetation model (Top-down Representation of Interactive Foliage and Flora Including Dynamics or TRIFFID) (Cox *et al.*, 2001; Meissner *et al.*, 2003), a land surface model (a simplified version of the Met Office Surface Exchange Scheme or MOSES) (Meissner *et al.*, 2003), an ocean ecosystem/biogeochemical model and an inorganic ocean carbon model (Schmittner *et al.*, 2008), and an oxic-only model of ocean sediment respiration (Archer, 1996; Eby *et al.*, 2009).

The MOM2 ocean component includes numerous physical parameterizations such as diffusive mixing along and between layers of different water density, eddy induced tracer transport based on Gent and McWilliams (1990), and the computation of tidally induced diapycnal mixing over rough seafloor topography (Simmons *et al.*, 2004). Radiocarbon ^{14}C and chlorofluorocarbons (CFCs) are used to track the ocean's ventilation to the atmosphere on decadal to millennial scales (Schmittner *et al.*, 2008).

The inorganic carbon cycle model is an Ocean Carbon-Cycle Intercomparison type (OCMIP-2) model while the ocean ecosystem/biogeochemical model is a nutrient-phytoplankton-zooplankton-detritus (NPZD) model based on Schmittner *et al.* (2005) with a fast microbial-induced nutrient recycling parameterization based on Schartau and Oschlies (2003). The NPZD model further includes two kinds of phytoplankton (nitrogen fixers and other phytoplankton (P_o)), nutrients such as phosphate (PO_4) and nitrate (NO_3), and tracers such as DIC, alkalinity, and oxygen (O_2).

The production of $CaCO_3$ in the model is calculated as

$$Pr(CaCO_3) = ((1 - ß)G(P_o)Z + \mu_{P2}P^2_o + \mu_z Z^2)(PIC^*:POC^*)R_{C:P} \qquad (6)$$

where $(1 - ß)G(P_o)Z$ represents the zooplankton grazing of the P_o phytoplankton type, $\mu_{P2}P^2_o$ represents the mortality of P_o phytoplankton, $\mu_z Z^2$ represents zooplankton mortality, $(PIC^*:POC^*)$, not to be confused with the PIC:POC rain ratio, is the production ratio of $CaCO_3$ to particulate organic carbon, and $R_{C:P}$ is the molar elemental ratio of carbon to phosphorus. As the vertically integrated $CaCO_3$ (PIC) production in the model is parameterized as a fixed ratio of the production of nondiazotrophic detritus (POC), the strength of the $CaCO_3$-pump is strongly influenced by the $PIC^*:POC^*$ parameter. The dissolution of $CaCO_3$ in the water column assumes an instantaneous sinking of the vertically integrated production (Schmittner *et al.*, 2008) with an e-folding depth of 6500m.

Phytoplankton growth rates and microbial remineralization rates in the biological carbon cycle component are assumed to increase with increasing temperature (Eppley, 1972; Schmittner *et al.*, 2008). Consequently, detrital production rates increase with increasing temperature as well due to enhanced biological carbon fixation. As $CaCO_3$ production in the model is parameterized as a fixed ratio of nondiazotrophic detrital production (PIC*:POC* parameter in equation 6), $CaCO_3$ production rates tend to increase along with detrital production rates in response to increasing sea surface temperatures resulting in a stronger vertical ocean alkalinity gradient (Schmittner *et al.*, 2008). To our knowledge only Schmittner *et al.* (2008) has previously described this "temperature effect" though a similar temperature dependence is expected in other ocean ecosystem models that parameterize $CaCO_3$ production as a function of temperature dependent primary production (Schmittner *et al.*, 2008).

The marine sediment component consists of 13 layers ranging from a few millimeters near the sediment surface to a few centimeters at the bottom of the domain at a depth of 10 cm. The penetration depth of POC into the surface sediment mixed layer in contact with overlying bottom waters, or "pore layer", is determined by the balance between the respiration rate constant and the sediment-mixing rate. Sediment $CaCO_3$ dissolution is regulated by the kinetics of diffusion of the dissolved reaction products from the sediments to the overlying water while the concentration and burial rates of sedimentary $CaCO_3$ are predicted using the PIC:POC rain ratio, dilutant burial rates (primarily clay and opal), and the reaction rate laws for both organic carbon and $CaCO_3$ (Archer, 1996). Only oxic metabolic dissolution of sedimentary $CaCO_3$ is simulated by

the sediment component and the effects of suboxic and anoxic metabolism are not accounted for (Eby *et al.*, 2009).

It should be noted that the UVic ESCM does not differentiate between the different polymorphs of $CaCO_3$ such as aragonite and calcite. Since the model does not properly resolve coastal processes where aragonite is produced we focus on the dependence of calcification on calcite saturation state only (Ω_{CaCO3}), which is a reasonable approximation given that approximately 90% of pelagic calcification is in the form of calcite (Fabry, 1990). Furthermore, mineral ballasting, which increases the efficiency of POC export to the deep sea, is not represented in the UVic ESCM therefore the model assumes an independence of organic and inorganic material fluxes to the deep ocean. Finally, for the purposes of this study, we have focused on the production dependence on Ω_{CaCO3}, and have not also introduced a dependence of dissolution on Ω_{CaCO3}.

3.2.2 Model Experimental Methodology

In this study, we present a series of transient model simulations from the year 1800 to 3500, so as to reasonably cover one full cycle of the oceanic meridional overturning circulation. In order to achieve a stable preindustrial climate, all simulations were individually integrated for 10 000 model years using fixed preindustrial boundary conditions. Transient runs are categorized in two suites of six simulations each. The first suite (suite S) was forced by the Intergovernmental Panel on Climate Change's "business-as-usual" SRES A2 CO_2 emissions scenario, reaching cumulative CO_2

44

emissions of 2166 Pg C by the year 2100. After 2100, emissions were set to zero for the duration of the simulations. The second suite (suite M) was forced by a "mitigation" emissions scenario, in which emissions peaked in the year 2020 and decreased to zero in year 2100, such that cumulative CO_2 emissions were capped at 1000 Pg C.

Terrestrial weathering of carbonate minerals and rock-bound organic carbon in the model is independent of climate change and is either set at a fixed rate or is diagnosed from sediment carbon burial. For simplicity, and in order to isolate changes in ocean alkalinity due to changes in $CaCO_3$ production from that resulting from fixed terrestrial weathering, the net change in terrestrial weathering was set to the net change in sedimentary $CaCO_3$ burial (net in (weathering) = net out (sediment $CaCO_3$ burial) in this study resulting in a conservation of carbon within the system.

Within each suite (S and M), we carried out six simulations, each with an increasing sensitivity of $CaCO_3$ production to changes in Ω_{CaCO3} (Figure 3.1). In the standard model configuration, $CaCO_3$ production is independent of saturation state and the PIC:POC production ratio used in the calculation of $CaCO_3$ production is fixed at a value of 0.018. This configuration was used for the "control" simulations S0 and M0 (see table 3.1). In the simulations with $CaCO_3$ production-saturation state dependence (S1 to S5 and M1 to M5 in Table 3.1), we introduced a Michaelis-Menten function to calculate the $CaCO_3$:nondiazotrophic detritus production ratio (PIC:POC) as a function of saturation state (Ω):

45

$$\frac{PIC}{POC} = \left(\frac{PIC}{POC}\right)_{max} \quad x \quad \frac{(\Omega - 1)}{K_{max} + (\Omega - 1)} \tag{7}$$

In this relationship, $(PIC/POC)_{max}$ is a specified maximum production ratio, and K_{max} is a half-saturation constant defining the value of $(\Omega - 1)$ for which PIC/POC equals one half of $(PIC/POC)_{max}$ (Gehlen *et al.*, 2007).
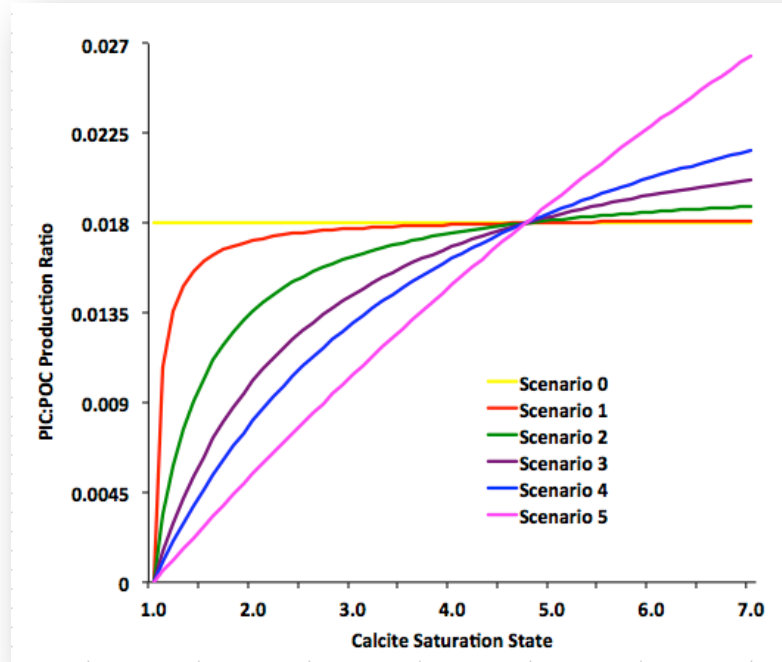
Figure 3.1 – CaCO$_3$:Particulate organic carbon production ratio dependence on calcite saturation state.

Table 3.1 summarizes the values of $(PIC:POC)_{max}$ and K_{max} used for each model version. We selected values of K_{max} ranging from 0.07 to 20 for each scenario in order to vary the shape of the PIC:POC vs. Ω_{CaCO3} function between no PIC:POC- Ω_{CaCO3}

46

response (scenario 0) to a near linear response (scenario 5), as illustrated in Figure 3.1. In order to calibrate each scenario so that the preindustrial PIC:POC production ratio was consistent with the unmodified model version (scenario 0), we back-calculated the value for (PIC:POC)$_{max}$ in each scenario using the preindustrial sea-surface calcite saturation state value of 4.78 from the standard model. In the subsequent transient simulations, changes to the PIC:POC production ratio over time brought about by ocean acidification varied according to the imposed calcification sensitivities.

Table 3.1 - Summary of Model Run Calibrations

Scenarios	Cumulative CO_2 Emissions by 2100 (Pg C)	K_{max}	(PIC:POC)$_{max}$	PIC:POC at Preindustrial Surface $\Omega_{calcite}$	Preindustrial Surface $\Omega_{calcite}$
S0		-	-		
S1		0.07	0.0183		
S2	2166 Pg C (all S)	0.5	0.0204		
S3		1.5	0.0251		
S4		3	0.0322		
S5		20	0.113		
M0		-	-	0.0180 (all)	4.78 (all)
M1		0.07	0.0183		
M2	1000 Pg C (all M)	0.5	0.0204		
M3		1.5	0.0251		
M4		3	0.0322		
M5		20	0.113		

3.3 Results

The distribution of $CaCO_3$ production is generally well simulated by the model and is broadly consistent with the global distribution of vertically integrated calcite production predicted by Gangsto *et al*. (2008) with low values in both central ocean gyres and polar waters and high values in the Indian Ocean and equatorial upwelling zones of the eastern Pacific and Atlantic Oceans (Figure 3.2).
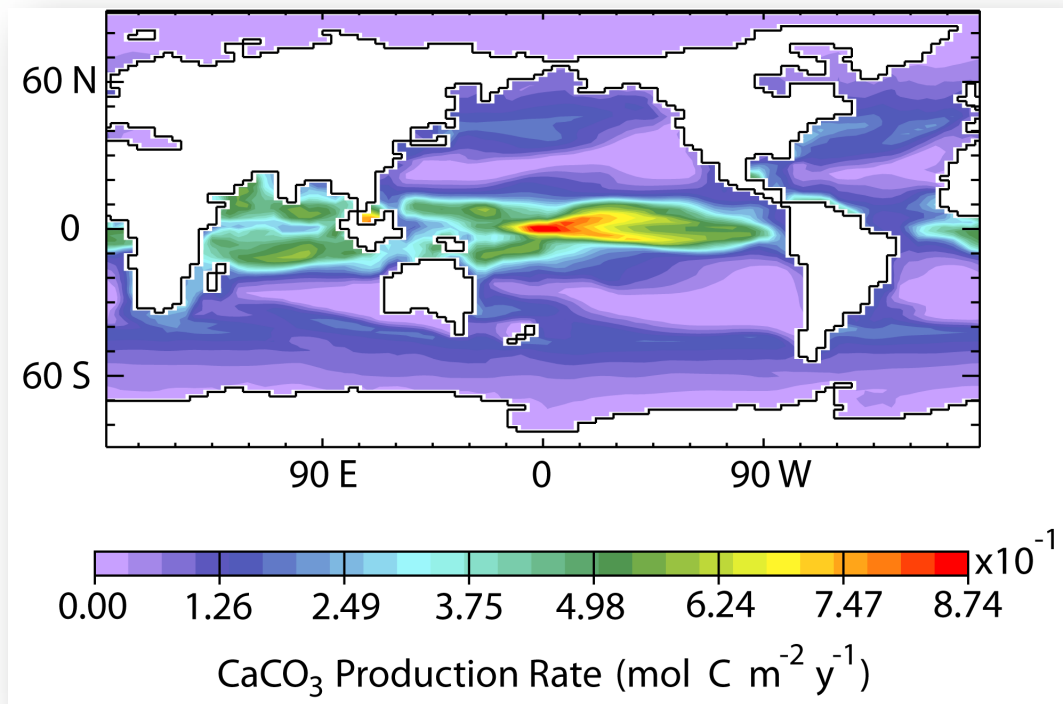
Figure 3.2 – Modeled distribution of preindustrial sea surface $CaCO_3$ production in the standard model version (simulation S0).

The model, however, simulates higher production rates in the central equatorial Pacific than the eastern equatorial Pacific compared to the findings of Gangsto *et al*.

(2008) due to the warmer sea surface temperatures predicted by the model in the central equatorial Pacific.

With increasing anthropogenic CO_2 emissions, the UVic ESCM simulated an increase in global ocean carbon uptake, thereby acting as a negative feedback on increasing atmospheric CO_2 concentrations. This increased ocean carbon uptake resulted in a decrease in surface ocean pH and Ω_{CaCO3}. In the standard version of the model, total ocean carbon increased by 522 Pg C by 2100 in response to "business-as-usual" CO_2 emissions (control run S0) resulting in decreases in globally averaged surface pH and surface Ω_{CaCO3} of 0.390 and 2.27 respectively relative to preindustrial conditions. (Figure 3.3a,c). In control run M0, total ocean carbon increased by 327 Pg C over the same timeframe resulting in a decrease in sea surface pH and Ω_{CaCO3} of 0.170 and 1.14 respectively relative to preindustrial conditions (Figure 3.3b,d). In both cases, after CO_2 emissions ceased in the year 2100, atmospheric CO_2 concentrations decreased over time, resulting in a slow recovery of ocean surface pH and saturation state. For the simulations with a calcification-saturation state dependence, the recovery of both pH and saturation state occurred slightly faster than in the control simulations.
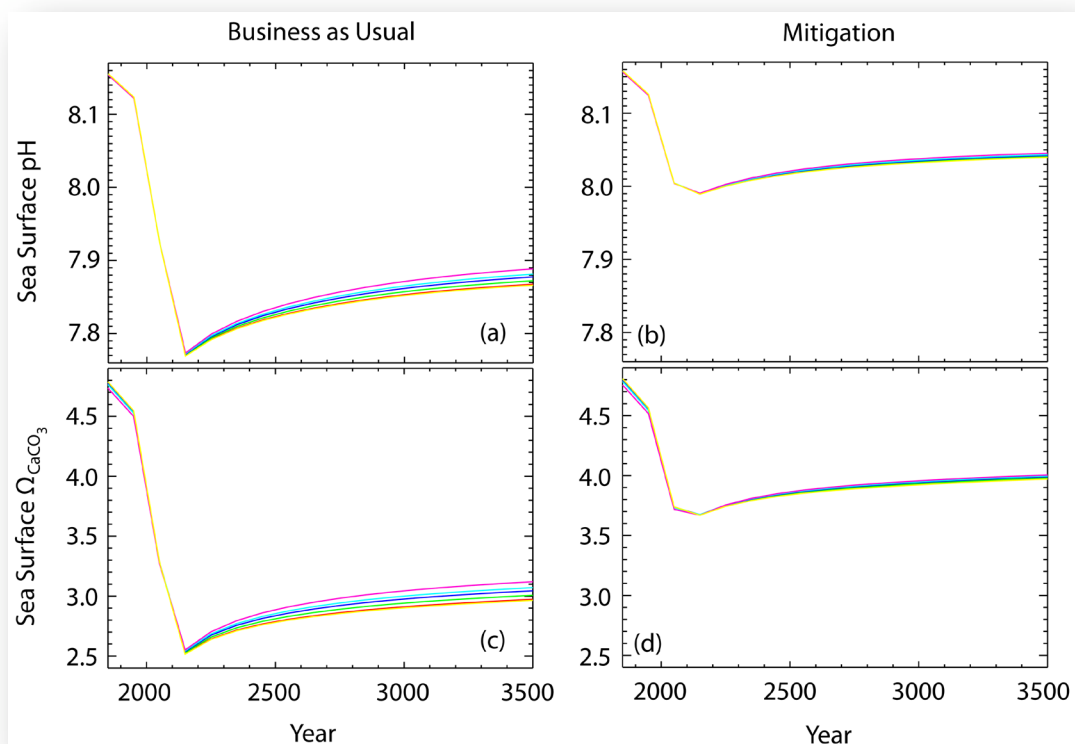
Figure 3.3 – Plot of change in globally averaged surface ocean pH (panels a,b) and calcite saturation state (panels c,d) for scenario 0 (yellow), scenario 1 (red), scenario 2 (green), scenario 3 (purple), scenario 4 (blue), and scenario 5 (pink) under a "business-as-usual" CO_2 emissions (panels a,c) and a "mitigation" CO_2 emissions scenario consisting of 1000 Pg C cumulative emissions (panels b,d) respectively.

In the standard version of the model (S0 and M0), by year 3500 the total sea surface $CaCO_3$ production rate increased by 0.142 Pg C y^{-1} in response to "business-as-usual" emissions, and by 0.0612 Pg C y^{-1} in the "mitigation" run. Incorporating $CaCO_3$ production dependency on Ω_{CaCO3} to the model, however, had a dramatic effect on the response of $CaCO_3$ production rates to increased ocean carbon uptake. As seen in Table 3.2 and Table 3.3, in response to the decrease in sea surface Ω_{CaCO3} brought on by anthropogenic CO_2 emissions, $CaCO_3$ production rate changes ranged from an increase of 0.133 Pg C y^{-1} (24.8%) in S1 to a decrease of 0.122 Pg C y^{-1} (18.6%) in S5. Similarly, in the "mitigation" runs, total sea surface $CaCO_3$ production rate changes ranged from an

50

increase of 0.0579 Pg C y^{-1} (10.7%) in M1 to a decrease of 0.0381 Pg C y^{-1} (5.8%) in

M5. In all cases, year 3500 production rates were reduced relative to the control runs (S0

and M0) as a result of the introduction of a dependency on saturation state (Figure 3.4).

Table 3.2 - Summary of the change in atmospheric and ocean output for years 1800 – 3500 for Suite S simulations. Values in column $S0_{1800}$ represent absolute output in the base model in year 1800. Subsequent columns show differences from 1800 to 3500 for each calcification sensitivity (S0 to S5).

	$S0_{1800}$	$S0_{3500-1800}$	$S1_{3500-1800}$	$S2_{3500-1800}$	$S3_{3500-1800}$	$S4_{3500-1800}$	$S5_{3500-1800}$
$CaCO_3$ Production Rate (Pg C y^{-1})	0.573	0.142	0.133	0.0749	0.0160	-0.0278	-0.122
$CaCO_3$ Sea Surface Export Rate (Pg C y^{-1})	0.569	0.141	0.132	0.0744	0.0159	-0.0276	-0.121
Sea Surface Alkalinity (Pg C)	175	-5.90	-5.76	-5.13	-4.36	-3.76	-2.44
Sea Surface DIC (Pg C)	152	3.93	4.03	4.46	4.99	5.41	6.31
Sea Surface pCO_2 (ppmv)	293	320	318	312	306	306	292
Total Ocean Carbon (Pg C)	37321	1108	1112	1127	1143	1155	1178
Total Atmospheric Carbon (Pg C)	602	675	671	658	645	635	615
Sea Surface Calcite Saturation State	4.79	-1.83	-1.82	-1.78	-1.74	-1.70	-1.62
Sea Surface pH	8.16	-0.290	-0.289	-0.284	-0.279	-0.275	-0.267

Table 3.3 - Summary of the change in atmospheric and ocean output for years 1800 – 3500 for Suite M simulations. Values in column $M0_{1800}$ represent absolute output in the base model in year 1800. Subsequent columns show differences from 1800 to 3500 for each calcification sensitivity (M1 to M5).

	$M0_{1800}$	$M0_{3500-1800}$	$M1_{3500-1800}$	$M2_{3500-1800}$	$M3_{3500-1800}$	$M4_{3500-1800}$	$M5_{3500-1800}$
$CaCO_3$ Production Rate (Pg C y^{-1})	0.572	0.0612	0.0579	0.0430	0.0222	0.00457	-0.0381
$CaCO_3$ Sea Surface Export Rate (Pg C y^{-1})	0.568	0.0607	0.0575	0.0427	0.0221	0.00453	-0.0378
Sea Surface Alkalinity (Pg C)	175	-2.60	-2.55	-2.38	-2.12	-1.90	-1.33
Sea Surface DIC (Pg C)	152	1.77	1.80	1.91	2.09	2.23	2.61
Sea Surface pCO_2 (ppmv)	292	105	105	104	103	102	99.5
Total Ocean Carbon (Pg C)	37321	574	574	577	581	584	592
Total Atmospheric Carbon (Pg C)	602	221	221	219	217	215	210
Sea Surface Calcite Saturation State	4.81	-0.842	-0.838	-0.826	-0.808	-0.793	-0.755
Sea Surface pH	8.16	-0.119	-0.119	-0.117	-0.116	-0.115	-0.112
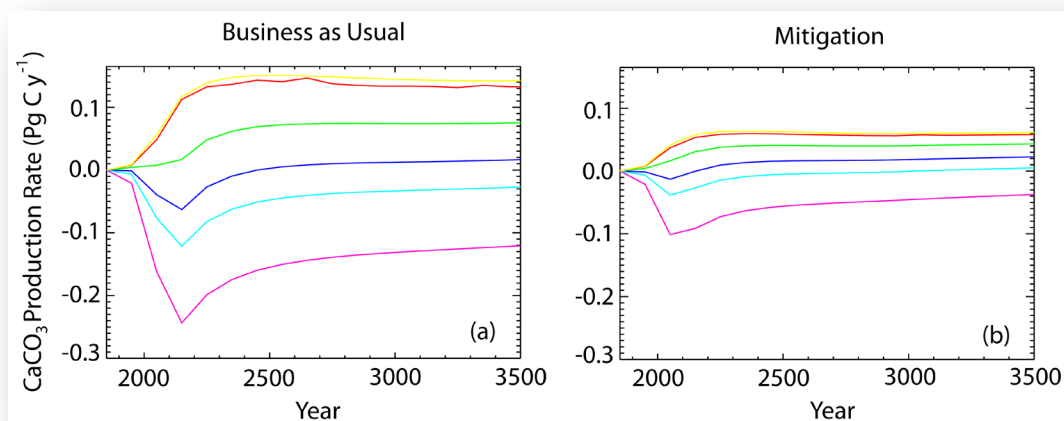
Figure 3.4 – Plot of the change in total sea surface CaCO$_3$ production rate for control scenario 0 (yellow), scenario 1 (red), scenario 2 (green), scenario 3 (purple), scenario 4 (blue), and scenario 5 (pink) under a) a "business-as-usual" CO$_2$ emissions scenario (Suite S) and b) under a 1000 Pg C cumulative CO$_2$ emissions scenario (Suite M).

In the highest sensitivity simulations (S5 and M5), the simulated reduction in CaCO$_3$ production rates increased total sea surface alkalinity and DIC relative to the control run by 3.46 Pg C and 2.38 Pg C respectively for simulation S5 and by 1.27 Pg C and 0.840 Pg C respectively for simulation M5. This change in sea surface alkalinity, generated by decreased biogenic calcification, offset the overall increase in globally averaged atmospheric pCO$_2$ by 28.0 ppmv and 5.38 ppmv in S5 and M5 respectively relative to control. Consequently, total ocean carbon at year 3500 was 70.0 Pg C (S5) and 18.2 Pg C (M5) higher than the control case, and total atmospheric carbon was 59.8 Pg C (S5) and 11.5 Pg C (M5) lower. Despite the increased ocean carbon uptake over the duration of the simulations, globally averaged surface ocean pH and Ω_{CaCO3} were greater relative to control by 0.0236 and 0.207 respectively for S5 and by 0.00714 and 0.0863 respectively for M5, suggesting a small decrease in the Revelle factor at the sea surface associated with decreased CaCO$_3$ production.

54

All runs simulated a vertical DIC and alkalinity gradient, due to increasing remineralization of POC and dissolution of PIC exported from the surface ocean with depth. In runs S1-S5 (and to a lesser extent in M1-M5), decreased $CaCO_3$ production and export rates from the surface to the deep ocean led to weaker vertical gradients of alkalinity and DIC with increased concentrations at the surface and decreased concentrations at depth (Figures 3.5 and 3.6). The greatest increases in alkalinity and DIC occurred in the top 1000 m of the ocean between 60°S and 60°N, particularly in the central ocean gyres at 30°S and 30°N, due to both advection and downwelling in those areas. Increased alkalinity and DIC was simulated throughout the water column in the Arctic Ocean due to the same processes, in addition to a small increase in $CaCO_3$ production and export from the surface to deeper ocean in that region. Throughout most of the ocean, DIC and alkalinity decreased at depth as a result of decreased export production, with the largest decreases evident at around 60°S and 45°N.
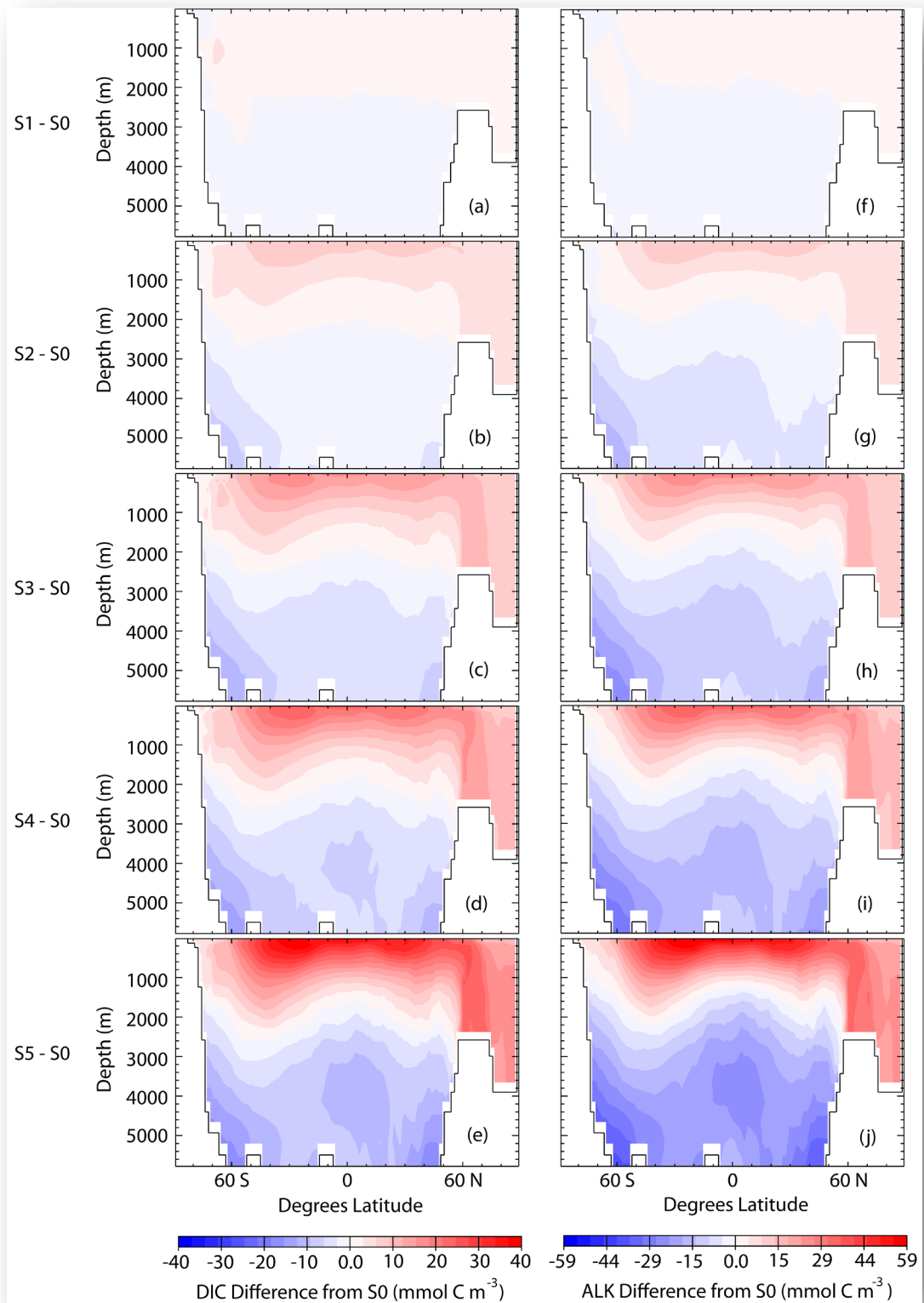
Figure 3.5 – Zonally averaged difference plots relative to control run S0 with respect to DIC for runs S1 to S5 (panels a to e respectively) and alkalinity for runs S1 to S5 (panels f to j respectively) in year 3500.
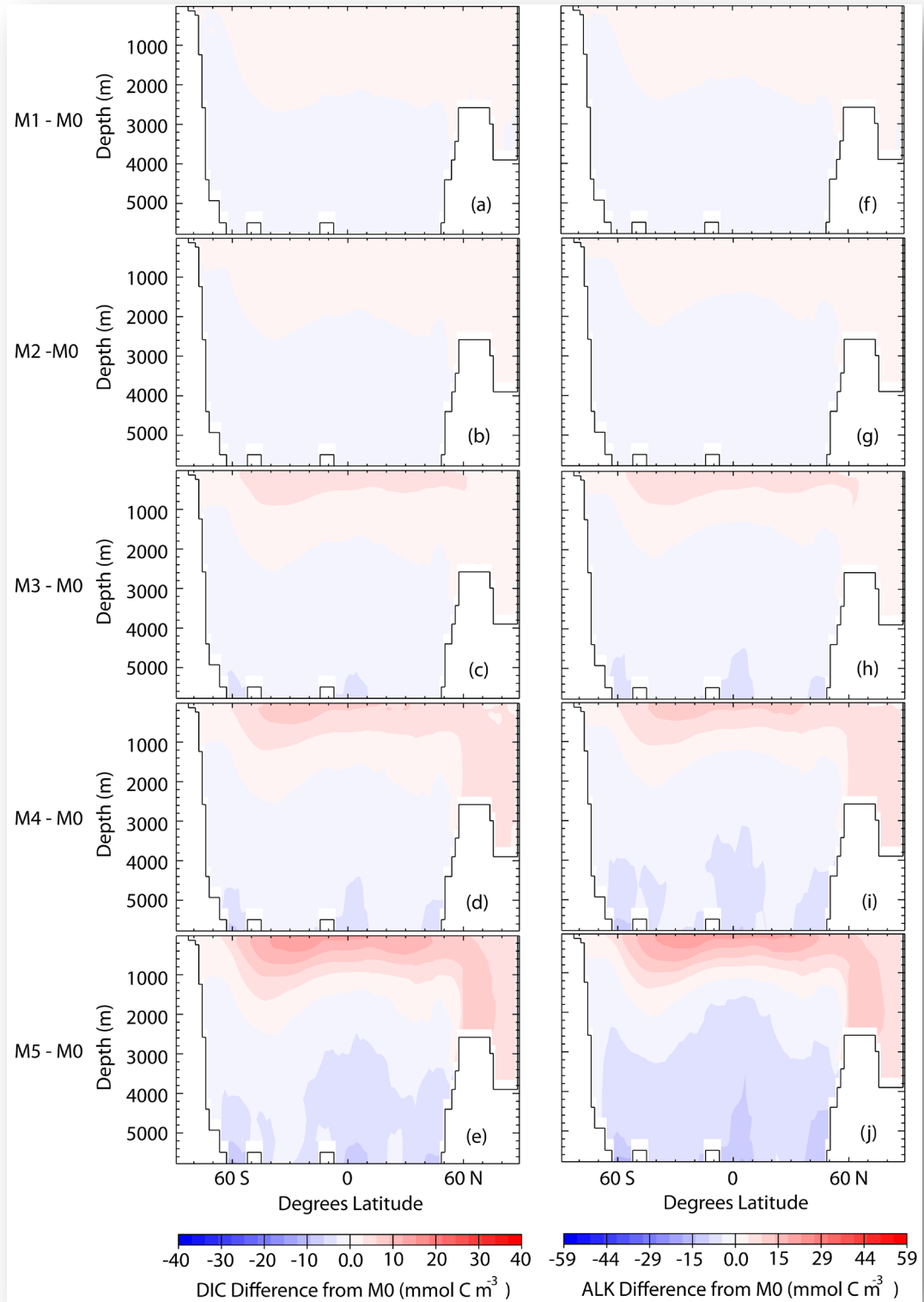
Figure 3.6 – Zonally averaged difference plots relative to control run M0 with respect to DIC for runs M1 to M5 (panels a to e respectively) and alkalinity for runs M1 to M5 (panels f to j respectively) in year 3500.

As shown in figure 3.7a, anthropogenic CO_2 emissions in the "business-as-usual"
S simulations led to a shoaling of the calcite saturation horizon to about 2000 m in the
Arctic Ocean, to 400m in the equatorial region, and to 250m in the high latitude Southern
oceans. In contrast, in the M simulations (Figure 3.7b), the model did not generate any
regions of undersaturation with respect to calcite by the year 3500. In runs S1-S5 (and
M1-M5), increased alkalinity led to small increases in saturation state at the surface, and
at depth in the Arctic Ocean, relative to the control runs. The greatest decreases in Ω_{CaCO3}
occurred at depth, particularly in the equatorial and North Atlantic regions, extending to
the Antarctic in the S-simulations, which reflect regions of decreased alkalinity relative to
the control (Figure 3.7c and d). Differences in areas of the ocean where $\Omega_{CaCO3} < 1$
between S simulations were small although areas of undersaturated water with respect to
calcite decreased in the deep Arctic and increased in the Southern oceans above 35°S as a
result of increasing $CaCO_3$ production rate sensitivity to changes in Ω_{CaCO3}.
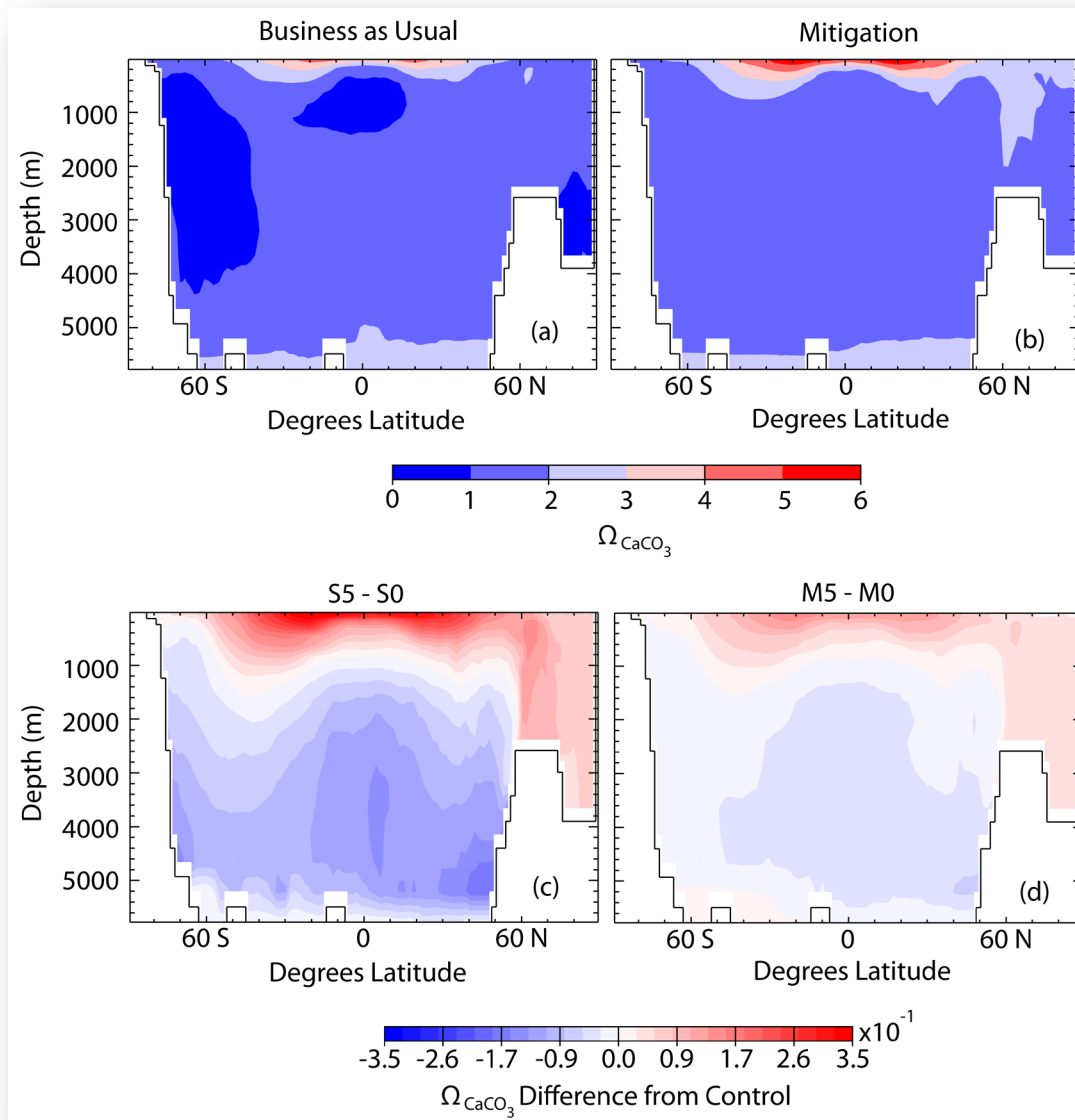
Figure 3.7 – Zonally averaged plots of calcite saturation state in year 3500 for a) simulation S0, b) simulation M0, c) S5-S0, and d) M5-M0 for a "business-as-usual" CO₂ emissions scenario (panels a,c) and a "mitigation" CO₂ emissions scenario consisting of 1000 Pg C cumulative emissions (panels b,d) respectively.

Table 3.4 - Summary of the change in rain ratio and sediment output for years 1800 – 3500 for Suite S simulations. Values in column $S0_{1800}$ represent absolute output in the base model in year 1800. Subsequent columns show differences from 1800 to 3500 for each calcification sensitivity (S0 to S5)..

	$S0_{1800}$	$S0_{3500-1800}$	$S1_{3500-1800}$	$S2_{3500-1800}$	$S3_{3500-1800}$	$S4_{3500-1800}$	$S5_{3500-1800}$
Rain Ratio Reaching Sediments (PIC:POC)	1.25	0.220	0.212	0.181	0.144	0.117	0.0605
Total Sediment Pore Layer $CaCO_3$ (Pg C)	1095	-31.7	-30.9	-37.3	-46.4	-54.2	-69.6
$CaCO_3$ Buried in Sediments (Pg C)	137104	216	212	201	189	183	174

Table 3.5 - Summary of the change in rain ratio and sediment output for years 1800 – 3500 for Suite M simulations. Values in column $M0_{1800}$ represent absolute output in the base model in year 1800. Subsequent columns show differences from 1800 to 3500 for each calcification sensitivity (M0 to M5)...

	$M0_{1800}$	$M0_{3500-1800}$	$M1_{3500-1800}$	$M2_{3500-1800}$	$M3_{3500-1800}$	$M4_{3500-1800}$	$M5_{3500-1800}$
Rain Ratio Reaching Sediments (PIC:POC)	1.25	0.0998	0.0977	0.0869	0.0716	0.0591	0.0316
Total Sediment Pore Layer $CaCO_3$ (Pg C)	1095	-20.6	-18.8	-19.9	-21.0	-21.2	-21.2
$CaCO_3$ Buried in Sediments (Pg C)	137104	216	217	218	223	229	249

In the control runs, the PIC:POC rain ratio reaching the ocean sediments increased over time as a result of the invasion of anthropogenic carbon and increased $CaCO_3$ production rates (by 0.220 in S0 and by 0.0998 in M0 – see Tables 3.4 and 3.5). In contrast, decreased $CaCO_3$ production and export in runs S1-S5 (and M1-M5) resulted in a decrease in the PIC:POC rain ratio reaching marine sediments, relative to the control runs, resulting in an overall reduction of $CaCO_3$ in the sediment pore layer (Tables 3.4 & 3.5). Relative to control, the globally averaged sediment rain ratio was 0.159 smaller at 3500 in S5 (Figure 3.8a) and 0.0682 smaller at 3500 in M5 (Figure 3.8d).

In all runs, increased sediment dissolution led to a decrease over time in the total $CaCO_3$-carbon in the sediment pore layer (Figure 3.8b and e). This decrease was enhanced at 3500 by 37.9 Pg C in S5 (Figure 3.8b) and by 0.540 Pg C in M5 (Figure 3.8e) as a result of the decreased rain ratio relative to the control runs. Changes also occurred in the deeper ocean sediments below the pore layer, the largest of the oceanic carbon reservoirs. In the S simulations, the mass of $CaCO_3$ sequestered in deeper sediments decreased by up to 42.0 Pg C relative to control (Figure 3.8c), but, in the M simulations, $CaCO_3$ sequestered in deeper sediments showed a different trend and increased by up to 33.0 Pg C relative to control (Figure 3.8f) due to less ocean acidification and less invasion of anthropogenic CO_2 to the deeper ocean compared to the S scenarios.
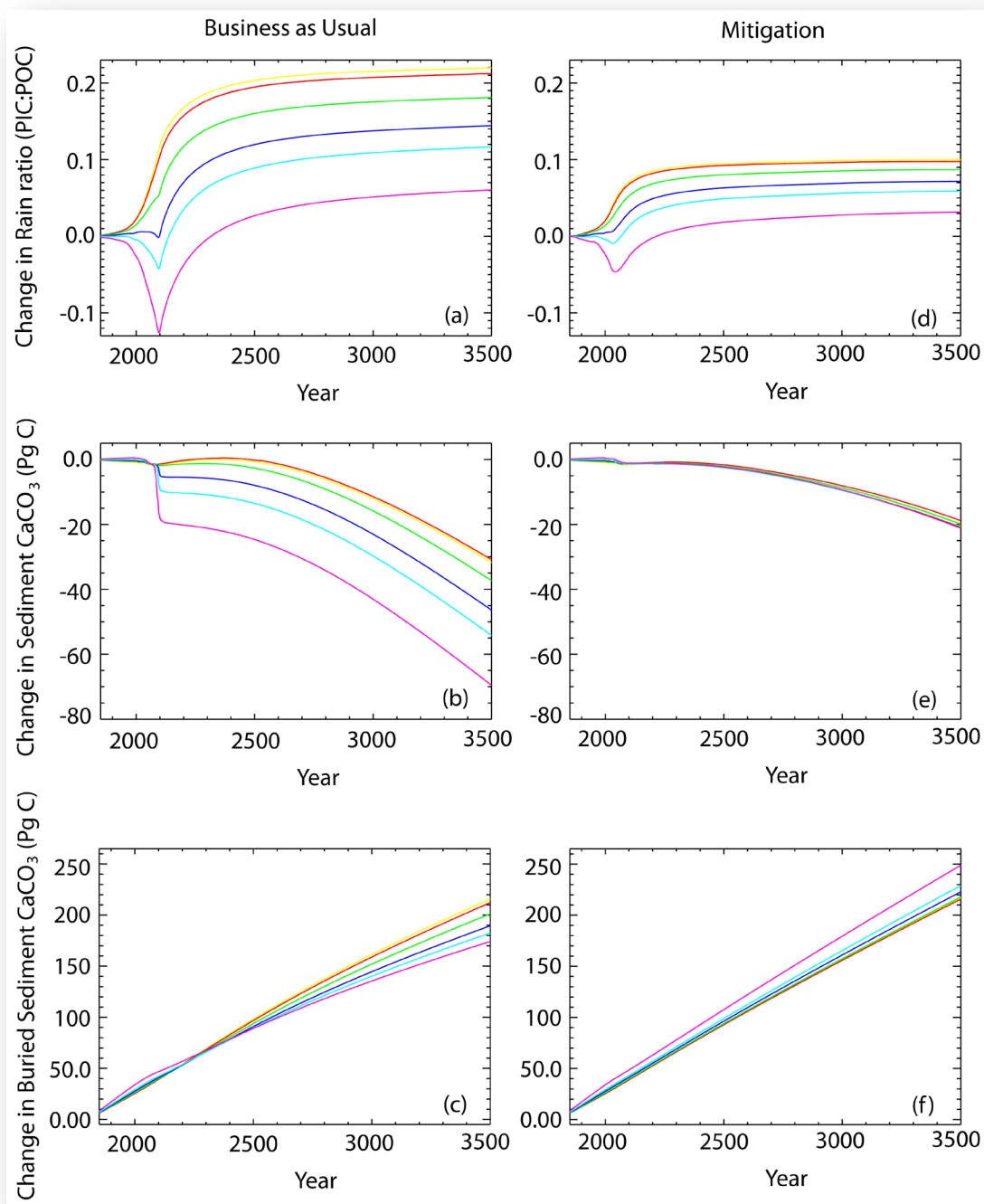
Figure 3.8 – Plots of the change in globally averaged sediment rain ratio (panels a,d), total CaCO$_3$-carbon in the sediment pore layer (panels b,e), and total CaCO$_3$ buried in deeper marine sediments (panels c, f) under a "business-as-usual" CO$_2$ emissions scenario (panels a,b,c) and a "mitigation" CO$_2$ emissions scenario consisting of 1000 Pg C cumulative emissions (panels d,e,f) respectively for control scenario 0 (yellow), scenario 1 (red), scenario 2 (green), scenario 3 (purple), scenario 4 (blue), and scenario 5 (pink).

3.4 Discussion

Our analysis of a range of different sensitivities of $CaCO_3$ production rates to changes in Ω_{CaCO3} under two different CO_2 emissions scenarios has yielded three main findings. First, including a $CaCO_3$ production-Ω_{CaCO3} dependency in the model led to large decreases in biogenic calcification with potentially important consequences for marine ecosystems. Second, these changes in calcification led to an enhancement of ocean carbon uptake providing a negative feedback on rising anthropogenic atmospheric CO_2. Third, increasing the sensitivity of the modeled $CaCO_3$ production-Ω_{CaCO3} relationship to reflect a range of calcification responses to ocean acidification leads to a small shift in carbon partitioning between atmosphere, ocean, and marine sediments and a weakening of the vertical alkalinity and DIC gradients. These findings suggest that despite the overall changes in atmospheric, ocean, and marine sediment carbon reservoirs being small, not including a Ω_{CaCO3} dependency on $CaCO_3$ production or taking into account the different responses of calcifying marine life to acidification would nevertheless add a source of error and uncertainty to model predictions.

The decrease in 22nd century surface ocean pH predicted by the UVic ESCM of 0.390 (representing nearly a 4-fold increase in hydrogen ions) is comparable with the 0.3 – 0.5 drop by 2100 predicted by Caldeira & Wickett (2005) under any of the SRES CO_2 emissions. This lends further credence to the concerns held by the scientific community regarding dangerous levels of ocean acidification unless anthropogenic CO_2 emissions are curtailed (SCBD, 2009). This is further highlighted by the much smaller changes in ocean pH of up to 0.170 pH units predicted under the "mitigation" CO_2 emissions

scenario (M simulations) where emissions were capped. Though the resulting change in Ω_{CaCO3} predicted by the model resulted in discreet zones of undersaturated waters with respect to calcite in the "business-as-usual" S simulations and none in the "mitigation" M simulations (as evidenced in Figure 3.7), it is important to note that these results are zonally averaged. Consequently, areas in the water column with Ω_{CaCO3} slightly less than 1 are averaged out and are not evident in the zonally averaged plots. Nevertheless, the greater degree of undersaturation with respect to calcite in the "business-as-usual" CO_2 emissions scenario (S simulations) relative to the "mitigation" CO_2 emissions scenario (M simulations) supports previous findings of significant areas of $CaCO_3$ undersaturation in the water column when pCO_2 exceeds 600 ppmv (Orr *et al*., 2005; Cao & Caldeira, 2008).

The increase in simulated $CaCO_3$ production rates in runs S0 and M0 with increasing atmospheric pCO_2 is the result of the temperature effect on detritus production. The UVic ESCM treats $CaCO_3$ production as a fraction of the nondiazotrophic detritus production although differences in remineralization and dissolution between $CaCO_3$ and detritus respectively are accounted for. As phytoplankton growth rates and detritus remineralization rates are temperature dependent in the model, warmer sea surface temperatures result in increased nutrient recycling in the euphotic zone which, in turn, result in increased primary production and detritus production. Consequently, in the absence of the Ω_{CaCO3}-effect (runs S0 and M0), $CaCO_3$ production increases proportionally with detritus production (Schmittner *et al*., 2008). In scenarios 1 and 2, the sensitivity of $CaCO_3$ production rates to changes in Ω_{CaCO3} was not high

enough to counteract this temperature effect so, although reduced relative to control, $CaCO_3$ production rates in these scenarios increased between years 1800 and 2100 despite increasing ocean acidification. In scenarios $3 - 5$, however, the sensitivity of $CaCO_3$ production rates to changes in Ω_{CaCO3} was high enough to counteract this temperature effect resulting in decreases in $CaCO_3$ production rates between years 1800 and 2100. This temperature effect also explains the higher preindustrial $CaCO_3$ production rates in the warmer central Pacific relative to the cooler eastern Pacific shown in Figure 3.3.

The modern $CaCO_3$ production rate of 0.6 Pg C y^{-1} predicted in the standard version of the model falls within the estimates of 0.6 -1.6 Pg C y^{-1} based on satellite and sediment trap data and of $0.4 – 1.8$ Pg C y^{-1} based on model predictions (Doney et al., 2009). As the $CaCO_3$ pump representation in the UVic ESCM is fairly crude (with no distinction between the different polymorphs of $CaCO_3$), it is difficult to make direct comparisons with the wide range of experimental results in the literature, particularly when experimental set-ups often differ greatly between studies (i.e. CO_2 forcings, model complexity, processes included/excluded, etc.). Nevertheless, broad parallels can still be drawn. In general, studies agree that increasing anthropogenic CO_2 emissions lead to a reduction in $CaCO_3$ production rates (Andrersson et al., 2006; Gangsto et al., 2008; Gangsto et al., 2011; Gehlen et al., 2007; Heinze, 2004; Ridgwell et al., 2006; SCBD, 2009). As previously stated, only the more sensitive calcification scenarios (S3-S5 and M3-M5) followed this decreasing trend in our simulations. The $CaCO_3$ production rate reduction of 20% for the year 2100 in run S4 is comparable to the 19% reduction in

CaCO$_3$ production rates simulated by Gangsto *et al*. (2008) for the year 2100 using the PISCES model, a model of similar complexity to the UVic ESCM, following the same "business-as-usual" CO$_2$ emissions scenario. This suggests that the standard model configuration (scenario 0) as well as scenarios 1 and 2, with weaker CaCO$_3$ production rate-Ω_{CaCO3} dependencies, are not consistent with experimental data or other model results such as (but not limited to) those of Riebesell *et al*. (2007) and Gangsto *et al*. (2011) respectively.

An important consequence of changing CaCO$_3$ production rates is the redistribution of carbon amongst the atmospheric, ocean, and sediment reservoirs with the magnitude of this redistribution increasing with decreasing CaCO$_3$ production rates. In all simulations, decreasing CaCO$_3$ production rates resulted in greater carbon uptake by the ocean and reduced carbon in the atmosphere. Between years 1800 and 3500, atmospheric pCO$_2$ only decreased by 2 - 28 ppmv in runs S1 – S5 (and by 0.3 – 5 ppmv in runs M1 – M5) relative to control, which supports the conclusions of Barker *et al*. (2003), Heinze *et al*. (2004), Gehlen *et al*. (2007) that the CO$_2$-CaCO$_3$ climate feedback is small. It is interesting to note that in all cases, ocean carbon increased more than the decrease in atmospheric carbon content. This extra carbon absorbed by the ocean actually originates in the terrestrial carbon pool, which lost said carbon to the atmosphere in response to climate warming. This suggests that the negative CO$_2$-CaCO$_3$ climate feedback may be weaker than would be suggested by simulations, which do not include an active terrestrial carbon component.

With the organic carbon pump remaining relatively unaffected by calcification changes, the changes in the simulated vertical DIC gradient relative to control can be attributed to changes in the export of surface ocean $CaCO_3$ to the deep ocean and the resulting lower PIC:POC rain ratios. The largest changes in surface alkalinity occur in the subtropical and tropical regions of the globe as in Ilynia *et al*. (2009), but, despite increases in surface alkalinity and reductions in $CaCO_3$ sediments there was little change in total ocean alkalinity in any runs relative to the standard model configuration. This suggests that changes in alkalinity in this study were the result of redistribution rather than net changes in net ocean alkalinity. This is expected considering that, with the terrestrial weathering rate of carbonate minerals equal to the net sediment $CaCO_3$ burial rate, the increases in surface alkalinity and the minute increases in total ocean alkalinity from reduced sediment sequestration relative to control are still very small compared to the total ocean alkalinity pool. Although, realistically, terrestrial weathering rates increase with climate change, the time-frame of our study is only 1700 years; given published estimates of the timeframe for the weathering of terrestrial $CaCO_3$ minerals and ocean carbonate compensation of $\gg 1700$ yrs (Lenton & Britton, 2006; Ridgwell & Hargreaves, 2007), increased terrestrial alkalinity input to the ocean and significant $CaCO_3$ sediment dissolution would only start to be noticeable.

The downward flux of $CaCO_3$ from the sediment pore layer followed the same pattern as $CaCO_3$ production rates seen in the S simulations and decreased relative to simulation S0 with greater sensitivity of $CaCO_3$ production to Ω_{CaCO3}. Consequently, the decrease in rain ratio contributed to both a reduction of $CaCO_3$ in the pore-layer and

68

decreased accumulation of $CaCO_3$ in deeper sediments. By contrast, the model simulated

a much smaller decrease in pore-layer $CaCO_3$ in the M simulations, and an increase in the

accumulation of buried $CaCO_3$ in runs M1-M5 relative to control M0. Barring

anthropogenic interference, the natural trend for the deep sediment carbon reservoir is to

increase as $CaCO_3$ export from the surface region ultimately leads to an accumulation of

$CaCO_3$ deposited on the sea floor and buried in sediments. In the M simulations,

increasing sensitivity of $CaCO_3$ production rates to Ω_{CaCO3} led to faster recovery of

Ω_{CaCO3}, pH, and sea-surface $CaCO_3$ production/export, which led to increased $CaCO_3$

burial, despite the opposing influence of decreased rain ratio. Consequently, $CaCO_3$ in

the pore-layer is still slightly decreased relative to control due to a smaller rain ratio but

the net burial of $CaCO_3$ in deeper sediments increased with increasing sensitivity of

$CaCO_3$ production to Ω_{CaCO3} relative to run M0.

We have shown here that representing different biogenic calcification responses

in coupled climate model predictions causes small but nevertheless important changes in

marine carbon cycling which, in turn, alters the fluxes between and the magnitudes of the

different carbon reservoirs of the Earth system. The changes in $CaCO_3$ production rates

between simulations for years 1800 - 3500 range from increases of 24.8% and 10.7% for

runs S0 and M0 respectively to decreases of 18.6% and 5.81% for runs S5 and M5

respectively. This wide range clearly illustrates the importance of choosing an optimal

sensitivity for $CaCO_3$ production rates to changes in Ω_{CaCO3}. Further research is required

in order to determine what model configuration best represents the variability in

calcification response between different species and strains of calcifiers, thereby further reducing this inherent uncertainty in model predictions of future climate change.

3.5 Conclusion

Ocean acidification brought on by increasing anthropogenic CO_2 emissions has been a growing concern in the scientific community. Its impact on calcifying marine life, which shows high inter-species variability, and the subsequent changes to marine carbon biogeochemical cycling lends a degree of uncertainty to climate model predictions of future climate change and the fate of anthropogenic CO_2. A number of modeling studies have attempted to address this uncertainty by assessing a range of biogenic calcification responses to changes in $CaCO_3$ saturation state rather than by relying on the representation of a single calcifying species as is commonly found in models of the ocean carbon cycle (Ridgwell *et al*. 2006, Ilynia *et al*. 2009, Gangsto *et al*. 2011). Our research has applied a broadly similar approach by implementing a new dependence of $CaCO_3$ production rates on calcite saturation state to a coupled carbon-climate model. We used six model scenarios: one control scenario where $CaCO_3$ production rates remained independent of saturation state and five calcification response scenarios with increasing sensitivity of production rates to saturation state changes. These scenarios were forced by two different CO_2 emissions scenarios allowing us to assess the differences in carbon partitioning between the various reservoirs, alkalinity and dissolved inorganic carbon distribution, and the strength of the ocean carbon sink.

By developing the UVic ESCM's representation of the marine $CaCO_3$ cycle and assessing a range of calcification scenarios, we have shown that including a $CaCO_3$ production-Ω_{CaCO3} dependency in the model leads to reduced $CaCO_3$ production rates with increasing atmospheric CO_2. This, in turn, leads to a small shift in carbon partitioning between atmosphere, ocean, and marine sediments relative to the respective sizes of the reservoirs and a weakening of the vertical ocean alkalinity and DIC gradients. Ocean carbon uptake, for example, is enhanced by reduced calcification thereby acting as a small negative feedback on rising anthropogenic atmospheric CO_2. Between the years 1800-3500, $CaCO_3$ production rates decreased by up to 18.6% under a "business-as-usual" scenario with cumulative CO_2 emissions of 2166 Pg C and by up to 5.81% forced by a "mitigation" scenario with cumulative CO_2 emissions of 1000 Pg C. By contrast, in the control runs without a $CaCO_3$ production-Ω_{CaCO3} dependence, calcification rates increased over the same time period by 24.8% in "business-as-usual" scenario and by 10.4% in the "mitigation" scenario due to sea surface warming.

The resulting increases in ocean carbon uptake of up to 70.0 Pg C and 18.2 Pg C led to reductions in atmospheric pCO_2 of up to 28.2 ppmv and 5.41 ppmv for the "business-as-usual" and "mitigation" scenarios respectively, suggesting an increasing negative feedback on atmospheric CO_2 with increasing $CaCO_3$ production-Ω_{CaCO3} sensitivity. Alkalinity and DIC generally increased at the surface and decreased with depth with changes in Ω_{CaCO3} resulting in most of the water column in the southern oceans poleward of 35ºS becoming undersaturated with respect to calcite by the year 3500. This result supports the growing body of evidence in the literature that the southern

oceans are one of the most sensitive marine regions to anthropogenic perturbation and will show the greatest changes in calcite saturation state in response to ocean acidification. Additionally, reductions in $CaCO_3$ production rates led to a small decreases in the PIC:POC rain ratio to the sediments, overall decreases in $CaCO_3$ in the sediment mixed layer and, in the "business-as-usual" scenario, resulted in decreased carbon sequestration in the marine sediment carbon pool of up to 42.0 Pg C. Carbon sequestration in the "mitigation" scenario, however, increased with increasing $CaCO_3$ production-Ω_{CaCO3} sensitivity providing yet another example of the benefits of curtailing our fossil fuel dependency.

Based on preliminary development of the UVic ESCM $CaCO_3$ component and our subsequent analysis of a range of biogenic calcification responses, we suggest that although the negative CO_2-calcification feedback is small, the effect of the $CaCO_3$ production-Ω_{CaCO3} relationship on the marine carbon cycle is still far-reaching and nevertheless provides a source of uncertainty in model predictions of future climate change. Given ongoing efforts to curtail cumulative anthropogenic CO_2 emissions, proper representation of long-term carbon-cycle processes in models grows ever more important in order to predict the millennial-scale legacy of current and future CO_2 emissions.

Acknowledgements

Chapter 4. Conclusion

Increasing concentrations of atmospheric carbon dioxide ($[CO_2]_{atm}$) resulting from anthropogenic CO_2 emissions has been shown to lead to ocean acidification and sea surface warming which, in turn, impact the biogeochemical cycling of carbon in the ocean and, ultimately, impact $[CO_2]_{atm}$ thus forming a feedback loop. Ocean acidification reduces the Ω_{CaCO3} leading to reduced $CaCO_3$ production and export rates. This, in turn, resulted in increased sea surface alkalinity and DIC concentrations, reduced PIC:POC rain ratios, increased ocean carbon uptake, and changes to sedimentary $CaCO_3$. Most models of the ocean carbon cycle use only one representative group of calcifying species. This, however, leads to a degree of uncertainty in model predictions as studies have shown that the calcification response to ocean acidification varies widely from species to species and even between different strains of the same species. A number of modeling studies have attempted to address this uncertainty (Ridgwell *et al*. 2006, Ilynia *et al*. 2009, and Gangsto *et al*. 2011) and their results have highlighted the need for more developed models of the marine carbon cycle.

My research is a contribution to the development of the representation of $CaCO_3$ in the UVic ESCM, an intermediate complexity coupled carbon-climate model. I have introduced a negative calcification-CO_2 feedback by implementing a dependency of $CaCO_3$ production rates on calcite saturation state, which observations have indicated shows a decreasing trend with increasing anthropogenic CO_2 emissions. The model was then run through a series of simulations running from the year 1800 to the year 3500 and forced by two 21st century CO_2 emissions scenarios. The control calcification scenarios

were represented by the standard version of the model where $CaCO_3$ production rates remained independent of $CaCO_3$ saturation state; the remaining five experimental simulations spanned a range of different calcification sensitivities to changes in saturation state. This allowed me to assess how different representative calcification responses and atmospheric CO_2 levels would affect alkalinity, dissolved inorganic carbon, and saturation state, as well as the magnitude of both the CO_2-calcification feedback and carbon partitioning between the various Earth system reservoirs.

My research has yielded three main findings. First, including a $CaCO_3$ production-Ω_{CaCO3} dependency in the model led to large decreases in biogenic calcification rates. Second, these reductions in calcification enhanced ocean carbon uptake thereby providing a negative feedback on rising anthropogenic atmospheric CO_2. Third, increasing the sensitivity of the modeled $CaCO_3$ production-Ω_{CaCO3} relationship to reflect a range of calcification responses to ocean acidification led to a small shift in carbon partitioning between atmosphere, ocean, and marine sediments and a weakening of the vertical alkalinity and DIC gradients. Although the reported changes in carbon partitioning between the atmospheric, terrestrial, ocean, and marine sediment reservoirs were small relative to the size of each respective reservoir, they nevertheless add uncertainty to model predictions that requires addressing. Improving the model's representation of $CaCO_3$ cycle processes will provide more dependable predictions of future climate change, marine carbon cycling, and the fate of anthropogenic CO_2.

This study has also highlighted several opportunities for further research. In this thesis project, I focused on the implementation of a $CaCO_3$ production- Ω_{CaCO3} dependency. An important next step would be to also implement a Ω_{CaCO3}-dependency on the dissolution of $CaCO_3$ exported from the surface layer to the deeper ocean. Such a dependency might further alter the vertical DIC and alkalinity gradients as well as the magnitude of the $CaCO_3$-CO_2 feedback. Most importantly, however, this would permit the UVic ESCM to differentiate between the different $CaCO_3$ polymorphs such as calcite and aragonite. Another opportunity would be to incorporate mineral ballasting into the model as it would not only alter the predicted DIC gradient but this process has the potential to increase the sea surface Revelle factor thereby offsetting the negative CO_2-$CaCO_3$ feedback on $[CO_2]_{atm}$. Further development of the terrestrial weathering process is also required in order to make terrestrial weathering dependent on climate change. Including this process would have a significant impact on ocean alkalinity, sediment $CaCO_3$ burial/dissolution, and the buffering capacity of the ocean. It would also be interesting to explore a wider range of anthropogenic CO_2 emissions scenarios, and to extend the time-frame of simulations to cover another several millennia into the future. Time and computational constraints preclude these steps within the scope of this project, but could potentially allow for the exploration of additional processes and feedbacks, particularly terrestrial weathering and calcium carbonate compensation, which become increasingly important on longer time scales that those considered here.

Although this study highlights the importance of model development it joins other studies in the literature in raising an important question. I have shown here that modeling

different calcification sensitivities to changes in $CaCO_3$ saturation state has small yet numerous impacts on atmosphere-ocean-sediment dynamics. However, it remains to be determined what model configuration best represents the variability in calcification response between different species and strains of calcifiers in order to reduce this inherent uncertainty in model predictions of future climate change. This merits further research and suggests that yet more advances in carbon-climate model development is required.

References

ARCHER, D. and E. MAIER-REIMER, (1994). Effect of deep-sea sedimentary calcite preservation on atmospheric CO_2 concentration. *Nature.* 367(6460): 260-263.

ARCHER, D. (1996). A data-driven model of the global calcite lysocline. *Global Biogeochem Cy.* 10(3): 511-526.

ARCHER, D.; H. KHESHGI, and E. MAIER-REIMER. (1997). Multiple timescales for neutralization of fossil fuel CO_2. *Geophys Res Lett.* 24(4): 405-08.

ARCHER, D.; H. KHESHGI, and E. MAIER-REIMER. (1998). Dynamics of fossil fuel CO_2 neutralization by marine $CaCO_3$. *Global Biogeochem Cy.* 12(2): 259-76.

ARMSTRONG, R.A.; C. LEE, J.I HEDGES, S. Honjo, and S.G WAKEHAM. (2002). A new, mechanistic model for organic carbon fluxes in the ocean based on the quantitative association of POC with ballast minerals. *Deep-Sea Res Pt II.* 49(1-3): 219-236.

ARMSTRONG, R.A.; M.L. PETERSON, C. LEE, and S.G. WAKEHAM. (2009). Settling velocity spectra and the ballast ratio hypothesis. *Deep-Sea Res Pt II.* 56(18): 1470-1478.

ANDERSSON, A. J.; F.T. MACKENZIE, and A. LERMAN. (2006). Coastal ocean CO_2-carbonic acid-carbonate sediment system of the Anthropocene. *Global Biogeochem Cy.* 20(1): GB1S92, doi:10.1029/2005GB002506.

BARKER, S.; J.A. HIGGINS, and H. ELDERFIELD. (2003). The future of the carbon cycle: review, calcification response, ballast and feedback on atmospheric CO_2. *Philos T Roy Soc A.* 361(1810): 1977-1998.

CAO, L.; K. CALDEIRA, and A.K. JAIN. (2007). Effects of carbon dioxide and climate change on ocean acidification and carbonate mineral saturation. *Geophys Res Lett.* 34(5): L05607, doi:2006GL028605.

CAO, L. and K. CALDEIRA. (2008). Atmospheric CO_2 stabilization and ocean acidification. *Geophys Res Lett.* 35(19): L19609, doi:10.1029/2008GL035072.

CALDEIRA, K. and M.E. WICKETT. (2005). Ocean model predictions of chemistry changes from carbon dioxide emissions to the atmosphere and ocean. *J Geophys Res – Oceans.* 110: C09S04, doi:10.1029/2004JC002671.

CHUCK, A.; T. TYRRELLl, I.J. TOTTERDELL, and P.M. HOLLIGAN. (2005). The oceanic response to carbon emissions over the next century: investigation using three ocean carbon cycle models. *Tellus B*. 57(1): 70-86.

COX, P.M. (2001). Description of the "TRIFFID" dynamic global vegetation model. *Hadley Center Technical Note 24*, Met Office, UK.

DE LA ROCHA, C. L. and U. PASSOW. (2007). Factors influencing the sinking of POC and the efficiency of the biological carbon pump. *Deep-Sea Res Pt II*. 54(5-7): 639-658.

DEPARTMENT OF ENERGY. (September 1994). Handbook of methods for the analysis of the various parameters of the carbon dioxide system in sea water; version 2. A.G. Dickson & C. Goyet, eds., ORNL/CDIAC-74.

DENMAN, K.L.; G. BRASSEUR, A. CHIDTHAISONG, P. CIAIS, P.M. COX, R.E. DICKINSON, D. HAUGLUSTAINE, C. HEINZE, E. HOLLAND, D. JACOB, U. LOHMANN, S. RAMACHANDRAN, P.L. DA SILVA DIAS, S.C. WOFSY, and X.ZHANG. (2007). Couplings between changes in the climate system and biogeochemistry. In: *Climate Change 2007: The Physical Science Basis. Contribution of Working Group I to the Fourth Assessment Report of the Intergovernmental Panel on Climate Change* [SOLOMON, S.; D. QIN, M. MANNING, Z. CHEN, M. MARQUIS, K.B. AVERYT, M. TIGNOR, and H.L. MILLER (eds.)]. Cambridge University Press, Cambridge, United Kingdom and New York, NY, USA.

DIMIZA, M.D.; M.V. TRIANTAPHYLLOU, and E. KRASAKOPOULOU. (2011). Coccolithophores (calcareous nannoplankton) distribution in the surface waters of the western Cretan Straits (South Aegean Sea): productivity and relation with the circulation pattern. *Hellenic Journal of Geosciences*. 45: 55-63.

DONEY, S.C. (2009). The consequences of human-driven ocean acidification for marine life. *Biology Reports Ltd.* 1(36): doi:10.3410/B1-36.

DONEY, S. C.; V.J. FABRY, R.A. FEELY, and J.A. KLEYPAS. (2009). Ocean acidification: The other CO_2 problem. *Ann Rev Mar Sci.* 1: 169-192.

EBY, M.; K. ZICKFELD, A. MONTENEGRO, D. ARCHER, K.J. MEISSNER, and A.J. WEAVER. (2009). Lifetime of Anthropogenic climate change: Millennial time scales of potential CO_2 and surface temperature perturbations. *J Climate.* 22(10): 2501-2511.

EPPLEY, R.W. (1972). Temperature and phytoplankton growth in the sea. *Fish. Bull*., 70, 1063-1085.

FABRY, V.J. (1990). Shell growth rates of pteropod and heteropod mollusks and aragonite production in the open ocean: Implications for the marine carbonate system. *J. Mar. Res*. 48: 209-222.

FABRY, V.J.; B.A. SEIBEL, R.A. FEELY, and J.C. ORR (2008). Impacts of ocean acidification on marine fauna and ecosystem processes. *ICES J. Mar. Sci*. 65: 414-432.

FALKOWSKI, P.; R.J. SCHOLES, E. BOYLE, J. CANADELL, D. CANFIELD, J. ELSER, N. GRUBER, K. HIBBARD, P. HÖGBERG, S. LINDER, F.T. MACKENZIE, B. MOORE III, T. PENDERSEN, Y. ROSENTHAL, S. SEITZINGER, V. SMETACEK, and W. STEFFEN. (2000). The global carbon cycle: A test of our knowledge of earth as a system. *Science.* 290(5490): 291-296.

FEELY, R.A.; R.H. BYRNE, J.G. ACKER, P.R. BETZER, C.T.A. CHEN, J.F. GENDRON, and M.F. LAMB. (1988). Winter-summer variations of calcite and aragonite saturation in the North Pacific. *Mar. Chem.* 25(3): 227-241.

FEELY, R.A.; C.L. SABINE, K. LEE, W. BERELSON, J. KLEYPAS, V.J. FABRY, F.J. MILLERO. (2004). Impact of anthropogenic CO_2 on the $CaCO_3$ system in the oceans. *Science.* 305(5682): 362-366.

FEELY, R.A.; C.L. SABINE, J,M HERNANDEZ-AYON, D. LANSON, and B. HALES. (2008). Evidence for upwelling of corrosive "acidified" water into the continental shelf. *Science*. 320(5882): 1490-1492.

FEELY, R.A.; S.C. DONEY, and S.R. COOLEY. (2009). Ocean Acidification: Present conditions and future changes in a high-CO_2 world. *Oceanography*. 22(4): 36-47.

GANGSTO, R.; M. GEHLEN, B. SCHNEIDER, L. BOPP, O. AUMONT, and F. JOOS. (2008). Modeling the marine aragonite cycle: changes under rising carbon dioxide and its role in shallow water $CaCO_3$ dissolution. *Biogeosciences.* 5(4): 1057-1072.

GANGSTO, R.; F. JOOS, and M. GEHLEN. (2011). Sensitivity of pelagic calcification to ocean acidification. *Biogeosciences*. 8(2): 433-458.

GEHLEN, M.; R. GANGSTO, B. SCHNEIDER, L. BOPP, Aumont, O., & Ethe, C. (2007). The fate of pelagic $CaCO_3$ production in a high CO_2 ocean: a model study. *Biogeosciences.* 4(4): 505-519.

GEHLEN, M.; L. BOPP, and O. AUMONT. (2008). Short-term dissolution response of pelagic carbonate sediments to the invasion of anthropogenic CO_2: A model study. *Geochem Geophy Geosy.* 9: Q02012, doi:10.1029/2007GC001756.

GENT, P.R. and J.C. MCWILLIAMS. (1990). Isopycnal mixing in ocean circulation models. *J Phys Oceanogr.* 20(1): 150-155.

HEINZE, C. (2004). Simulating oceanic $CaCO_3$ export production in the greenhouse. *Geophys Res Lett.* 31(16): L16308, doi:10.1029/2004GL020613.

HOFMANN, M. and H. SCHELLNHUBER. (2009). Oceanic acidification affects marine carbon pump and triggers extended marine oxygen holes. *Proc. Nat. Acad. Sci.* 106(9): 3017-3022.

IGLESIAS-RODRIGUEZ, M.D.; P.R. HALLORAN, R.E.M. RICKABY, I.R. HALL, E. COLMENERO-HIDALGO, J.R. GITTINS, D.R.H. GREEN, T. TYRRELL, S.J. GIBBS, P. VON DASSOW, E. REHM, E.V. ARMBRUST, and K.P, BOESSENKOOL. (2008). Phytoplankton calcification in a high-CO_2 world. *Science.* 320(5874): 336-340.

ILYNIA, T.; R.E. ZEEBE, E. MAIER-REIMER, and C. HEINZE. (2009). Early detection of ocean acidification effects on marine calcification. *Global Biogeochem Cy.* 23: GB1008, doi:10.1029/2008GB003278.

INTER-ACADEMY PANEL ON INTERNATIONAL ISSUES (IAP). (2009). Statement on Ocean Acidification. Endorded, June 2009. Retrieved on 19-Jan-2010 from http://interacademies.net/Object.File/Master/9/075/Statement_RS1579_IAP_05.09final2.pdf.

ITO, T. and M.J. FOLLOWS. (2003). Upper ocean control on the solubility pump of CO_2. *J Mar Res.* 61(4):461–489.

KLAAS, C. and D. ARCHER. (2002). Association of sinking organic matter with various types of mineral ballast in the deep sea: implications for the rain ratio. *Global Biogeochem Cy.* 16(4): 1116, doi 10.1029/2001GB001765.

KUILE, B.; J. EREZ, E. PADAN. (1989). Mechanisms for the uptake of inorganic carbon by two species of symbiont-bearing foraminifera. *Mar Biol.* 103(2): 241-251.

LENTON, T. M. and C. BRITTON. (2006). Enhanced carbonate and silicate weathering accelerates recovery from fossil fuel CO_2 perturbations. *Global Biogeochem Cy.* *20*(3): GB3009, doi:10.1029/2005GB002678.

LE QUÉRÉ, C.; M.R. RAUPACH, J. G CANADELL, G. MARLAND, L. BOPP, P. CIAIS, T.J. CONWAY, S.C. DONEY, R.A. FEELY, P. FOSTER, P. FRIEDLINGSTEIN, K. GURNEY, R.A. HOUGHTON, J.I. HOUSE, C. HUNTINGFORD, P.E. LEVY, M.R. LOMAS, J, MAJKUT, N. METZL, J.P. OMETTO, G.P. PETERS, I.C. PRENTICE, J.T. RANDERSON, S.W. RUNNING, J.L. SARMIENTO, U. SCHUSTER, S.SITCH, T. TAKAHASHI, N. VIOVY, G.R. VAN DER WERF, AND F.I. WOODWARD. (2009). Trends in the sources and sinks of carbon dioxide. *Nature Geosci.*, 2: 831-836, doi: 10.1038/NGEO689.

MATTHEWS, H.D.; L. CAO, and K. CALDEIRA. (2009). Sensitivity of ocean acidification to geoengineered climate stabilization. *Geophys Res Lett.* 36: L10706, doi:10.1029/2009GL037488.

MEISSNER, K.J.; A.J. WEAVER, H.D. MATTHEWS, and P.M. COX. (2003). The role of land-surface dynamics in glacial inception: a study with the UVic Earth System Climate Model. *Clim. Dynam.* 21: 515–537.

MONACO DECLARATION. (October 2008). Second International Symposium on the Ocean in a High-CO2 World, Monaco. Retrieved on 19-Jan-2010 from http://ioc3.unesco.org/oanet/Symposium2008/MonacoDeclaration.pdf.

MORSE, J.W.; A.J. ANDERSSON, and F.T. MACKENZIE. (2006). Initial responses of carbonate-rich shelf sediments to rising atmospheric pCO_2 and "ocean acidification": role of high Mg-calcites. *Geochim Cosmochim Ac.* 70(23): 5814-5830.

MUCCI, A. (1983). The solubility of calcite and aragonite in seawater at various salinities, temperatures, and one atmosphere total pressure. *Am J Sci.* 283: 780-799.

ORR, J. C.; V.J. FABRY, O. AUMONT, L. BOPP, S.C. DONEY, R.A. FEELY, A. GNANADESIKAN, N. GRUBER, A. ISHIDA, F. JOOS, R.M. KEY, K. LINDSAY, E. MAIER-REIMER, R. MATEAR, P. MONFRAY, A. MOUCHET, R.G. NAJJAR, G. PLATTNER, K.B. RODGERS, C.L. SABINE, J.L. SARMIENTO, R. SCHLITZER, R.D. SLATER, I.J. TOTTERDELL, M. WEIRIG, Y. YAMANAKA, and Y. YOOL. (2005). Anthropogenic ocean acidification over the twenty-first century and its impact on calcifying organisms. *Nature.* 437(7059): 681-686.

RAVEN, J. A., and P.G. FALKOWSKI. (1999). Oceanic sinks for atmospheric CO_2. *Plant Cell Environ.* 22(6): 741-755.

RAHMSTORF, S. (2002). Ocean circulation and climate during the past 120,000 years. *Nature.* 419(6903): 207-214.

REVELLE, R.; H.E. SUESS. (1957). Carbon dioxide exchange between atmosphere and ocean and the question of an increase of atmospheric CO_2 during past decades, *Tellus*, 9: 18-27.

RIDGWELL, A.; I. ZONDERVAN, J.C. HARGREAVES, J. BIJMA, and T.M. LENTON. (2006). Significant long-term increase of fossil fuel CO_2 uptake from reduced marine calcification. *Biogeosci Discuss.* 3(6): 1763-1780.

RIDGWELL, A., and J.C. HARGREAVES. (2007). Regulation of atmospheric CO_2 by deep-sea sediments in an Earth system model. *Global Biogeochem Cy.* 21(2): GB2008, doi:10.1029/2006GB002764.

RIEBESELL, U.; I. ZONDERVAN, B. ROST, P.D. TORTELL, R.E. ZEEBE, and F.M.M. MOREL. (2000). Reduced calcification of marine plankton in response to increased atmospheric CO_2. *Nature.* 407(6802): 364-367.

RIEBESELL, U.; K.G. SCHULZ, R.G.J. BELLERBY, M. BOTROS, P. FRITSCHE, M. MEYERHOFER, C. NEILL, G. NONDAL, A. OSCHLIES, J. WOHLERS, and E. ZÖLLNER. (2007). Enhanced biological carbon consumption in a high CO_2 ocean. *Nature.* 450(7169): 545-548.

SABINE, C.L; R.A. FEELY, N. GRUBER; R.M. KEY; K. LEE; J.L. BULLISTER; R. WANNINKHOF, C.S. WONG; D.W.R. WALLACE; BRONTE TILBROOK; F.J. MILLERO; T. PENG; A. KOZYR; T. ONO; A. RIOS. (2004). The oceanic sink for anthropogenic CO_2, *Science*, 350(5682): 367-371.

SARMIENTO, J.L and N. GRUBER. (2006). *Ocean biogeochemical dynamics*. Princeton University Press, New Jersey, USA, 526 pages.

SECRETARIAT OF THE CONVENTION ON BIOLOGICAL DIVERSITY (2009). Scientific Synthesis of the Impacts of Ocean Acidification on Marine Biodiversity. *Montreal, Technical Series No. 46*, 61 pages.

SCHARTAU, M., and A. OSCHLIES. (2003). Simultaneous data-based optimization of a 1D-ecosystem model at three locations in the North Atlantic. Part 1: Method and parameter estimates, *J Mar Res.* 61: 765-793.

SCHMITTNER, A.; A. OSCHLIES, X. GIRAUD, M. EBY, and H.L. SIMMONS. (2005). A global model of the marine ecosystem for long term simulations: Sensitivity to ocean mixing, buoyancy forcing, particle sinking and dissolved organic matter cycling, *Global Biogeochem Cy.* 19: GB3004, doi:10.1029/2004GB002283.

SCHMITTNER, A.; A. OSCHLIES, H.D. MATTHEWS, and E.D. GALBRAITH. (2008). Future changes in climate, ocean circulation, ecosystems, and biogeochemical cycling simulated for a business-as-usual CO_2 emission scenario until year 4000 AD. *Global Biogeochem Cy.* 22(1): GB1013, doi:10.1029/2007GB002953.

SIMMONS, H.L.; S.R. JAYNE, L.C. ST.LAURENT, and A.J. WEAVER. (2004). Tidally driven mixing in a numerical model of the ocean general circulation, *Ocean Model.* 6 (3-4): 245-263.

SUNDQUIST, E.T. (2007). Geologic analogs: their value and limitations in carbon dioxide research. In: *The Changing Carbon Cycle: A Global Analysis* [TRABALKA, J.R. and D.E. REICHLE (eds.)]. Springer-Verlag, New York, 371-402.

TAKAHASHI, T.; J. OLAFSSON, J.G. GODDARD; D.W. CHIPMAN, and S.C. SUTHERLAND. (1993). Seasonal variation of CO2 and nutrients in the high-latitude surface oceans: a comparative study. *Global Biogeochem Cy.* 7(4):843-878.

TURLEY, C.; J.C. BLACKFORD, S. WIDDICOMBE, D. LOWE, P.D. NIGHTINGALE, A.P. REES. (2006). Reviewing the impact of increased atmospheric CO_2 on oceanic pH and the marine ecosystem. In: SCHELLNHUBER, H.J.; W. CRAMER, N. NAKICENOVIC, T. WIGLEY, G. YOHE (Eds.), Avoiding Dangerous Climate Change, 8. Cambridge University Press, Cambridge, pp. 65–70.

TYRRELL, T. (2008). Calcium carbonate cycling in future oceans and its influence on future climates. *J Plankton Res. 30*(2): 141-156.

WEAVER, A.J.; M. EBY, E.C. WIEBE, C.M. BITZ, P.B. DUFFY, T.L. EWEN, A.F. FANNING, M.M. HOLLAND, A. MACFADYEN, H.D. MATTHEWS, K.J. MEISSNER, O. SAENKO, A. SCHMITTNER, H. WANG, AND M. YOSHIMORI. (2001). The UVic Earth System Climate Model: Model description, climatology and applications to past, present and future climates. *Atmos Ocean*. 39: 361–428.

WOLF-GLADROW, D. A.; U. RIEBESELL; S. BURKHARDT, and J. BIJMA. (1999). Direct effects of CO_2 concentration on growth and isotopic composition of marine plankton. *Tellus B.* 51(2): 461-476.

ZACHOS, J.C.; U. RÖHL; S.A. SCHELLENBERG; A. SLUIJS; D.A. HODELL; D.C. KELLY; E. THOMAS; M. NICOLO; I. RAFFI; L.J. LOURENS; H. MCCARREN and D. KROON. (2005). Rapid acidification of the ocean during the Paleocene-Eocene thermal maximum. *Science*. 308(5728): 1611-1615.

ZEEBE, R.E. and D.A. WOLF-GLADROW (2001). CO_2 in seawater: equilibrium, kinetics, isotopes. *Vol. 65 of Elsevier Oceanography Book Series*, Elsevier Science Publishing, Amsterdam, The Netherlands.

ZEEBE, R. E. and P. WESTBROEK. (2003). A simple model for the $CaCO_3$ saturation state of the ocean: The "Strangelove", the "Neritan", and the "Cretan" Ocean. *Geochem Geophy Geosy.* 4*(12)*: doi:10.1029/2003GC000538.

ZEEBE, R.E. and J.C. ZACHOS. (2007), Reversed deep-sea carbonate ion basin gradient during Paleocene-Eocene thermal maximum. *Paleoceanography*. 22: PA3201, doi:10.1029/2006PA001395.

ZEEBE, R. E.; J.C. ZACHOS, K. CALDEIRA, and T. TYRRELL. (2008). Oceans - Carbon emissions and acidification. *Science.* 321(5885): 51-52.

ZHONG, S.J. and A. MUCCI. (1993). Calcite precipitation in seawater using a constant addition technique – a new overall reaction kinetic expression. *Geochim Cosmochim Ac.* 57(7): 1409-1417.

ZONDERVAN, I.; R.E. ZEEBE, B. ROST, and U. RIEBESELL. (2001). Decreasing marine biogenic calcification: A negative feedback on rising atmospheric pCO_2. *Global Biogeochem Cy. 15*(2): 507-516.